ARMY RESEARCH LABORATORY

Classical Gradual-Channel Modeling of Graphene Field-Effect Transistors (FETs)

by Frank Crowne

ARL-TR-5281 **August 2010**

NOTICES

Disclaimers

The findings in this report are not to be construed as an official Department of the Army position unless so designated by other authorized documents.

Citation of manufacturer's or trade names does not constitute an official endorsement or approval of the use thereof.

Destroy this report when it is no longer needed. Do not return it to the originator.

Army Research Laboratory
Adelphi, MD 20783-1197

ARL-TR-5281 **August 2010**

Classical Gradual-Channel Modeling of Graphene Field-Effect Transistors (FETs)

Frank Crowne
Sensors and Electron Devices Directorate, ARL

REPORT DOCUMENTATION PAGE	Form Approved OMB No. 0704-0188

1. REPORT DATE *(DD-MM-YYYY)*	2. REPORT TYPE	3. DATES COVERED (From - To)
August 2010	Progress	

4. TITLE AND SUBTITLE	5a. CONTRACT NUMBER
Classical Gradual-Channel Modeling of Graphene Field-Effect Transistors (FETs)	5b. GRANT NUMBER
	5c. PROGRAM ELEMENT NUMBER

6. AUTHOR(S)	5d. PROJECT NUMBER
Frank Crowne	5e. TASK NUMBER
	5f. WORK UNIT NUMBER

7. PERFORMING ORGANIZATION NAME(S) AND ADDRESS(ES)	8. PERFORMING ORGANIZATION REPORT NUMBER
U.S. Army Research Laboratory ATTN: RDRL-SER-E 2800 Powder Mill Road Adelphi, MD 20783-1197	ARL-TR-5281

9. SPONSORING/MONITORING AGENCY NAME(S) AND ADDRESS(ES)	10. SPONSOR/MONITOR'S ACRONYM(S)
	11. SPONSOR/MONITOR'S REPORT NUMBER(S)

12. DISTRIBUTION/AVAILABILITY STATEMENT

Approved for public release; distribution unlimited.

13. SUPPLEMENTARY NOTES

14. ABSTRACT

This technical report describes initial efforts, as part of the new Strategic Technology Initiative (STI) on carbon electronics, to model and simulate the performance of graphene field-effect transistors (FETs) using macroscopic descriptions that are classical for semiconductor devices. It is argued that the underlying physics that differentiates these devices from their normal semiconductor-based counterparts is most clearly revealed by non-computer-intensive descriptions that allow the designer to compare their behavior with that of their well-studied semiconductor counterparts. Because it admits a reasonable description of both the lateral and vertical field and transport functionality of the FET structure, the gradual-channel approximation is key to this approach. The availability of closed-form solutions to the problem within this approach, in turn, allows small-signal and microwave parameters to be calculated quickly and transparently.

15. SUBJECT TERMS

Graphene, FET, gradual channel, I-V curve, stability

16. SECURITY CLASSIFICATION OF:			17. LIMITATION OF ABSTRACT	18. NUMBER OF PAGES	19a. NAME OF RESPONSIBLE PERSON
a. REPORT	b. ABSTRACT	c. THIS PAGE			Frank Crowne
Unclassified	Unclassified	Unclassified	UU	78	19b. TELEPHONE NUMBER (*Include area code*) (301) 394-5759

Standard Form 298 (Rev. 8/98)
Prescribed by ANSI Std. Z39.18

Contents

List of Figures

1. Introduction

Over the past 60 years, a large number of papers have been written about the properties of graphene (*1*), due not only to its defining characteristic as the ultimate two-dimensional (2-D) electronic system but also to its unique band structure and the strongly covalent features of its atomic bonding, properties that it inherits from the semimetal graphite. Indeed, the earliest papers on graphene (*2*) treat the material as an idealized version of graphite, i.e., a perfect monolayer of carbon with a hexagonal graphite structure. Despite the apparent simplicity of this "single-layer graphite" model, the picture of graphene that evolved from these papers is one of extreme complexity. This is because the relative simplicity of its constituents—atoms of a light-atomic-number element, carbon, in a simple high-symmetry lattice—favors the application of a high-powered many-body analysis of the electronic degrees of freedom, which, in turn, predicts ferromagnetism, superconductivity, charge-density waves, quantum Hall effects, and other even more novel phenomena. However, in view of the extreme difficulty of creating such monolayer structures, many of the theoretical results obtained from this extensive research have been considered irrelevant by technologists. As has often happened in the past, experimental advances have now overcome the fabrication difficulties to the point that the reality of graphene as an object of laboratory study is beyond question, and so these theoretical predictions can be put to the test.

On the other hand, the technological implications of graphene's physics—its monatomic nature, excellent electron/hole transport properties, and mechanical strength among others—have driven an effort to create devices that (it is claimed) could rival silicon-based transistors, and possibly harness the various exotic properties of the material that have been foreseen by theorists. At this time, there are still formidable obstacles to making graphene devices and circuits on the scale of those based on any standard semiconductor-based material, let alone highly evolved silicon devices. However, interest in graphene devices has now reached a point where models of such devices are needed that describe the terminal characteristics of circuit components without the need to track the interior details of the device function. The availability of fast computer simulations of ordinary semiconductor devices has motivated efforts to incorporate such details in the device computations, but the problem of long running times for codes based on these simulations has not been solved.

In this report, I argue that, rather than imitating those models of standard semiconductor-based devices that incorporate massive ab initio computer calculations—metal-oxide semiconductor field-effect transistors (MOSFETs), high electron mobility transistors (HEMTs), metal semiconductor field-effect transistors (MESFETs), and their ilk—the development of graphene device models should be evolutionary, i.e., the models should first mimic the simplest standard models. As a first step in this program, I discuss the simplest semiconductor device—the field-

effect transistor (FET)—treated at the lowest level of device modeling, i.e., Shockley's gradual-channel model. My choice of FETs is driven by ongoing interest in radio frequency (RF) devices here at the U.S. Army Research Laboratory (ARL) and the mature understanding of the high-frequency behavior of FETs in general. In the course of this analysis, I highlight places where the unique properties of graphene affect the predicted terminal characteristics and S-parameters of a possible graphene FET.

2. Description of Gradual-Channel Modeling

This type of device modeling, which was developed by Shockley (*3*) in the pre-computer era, is based on highly idealized pictures of the interior fields and currents of the device under study. For a FET, the standard geometry is shown in figure 1. The device consists of an insulating substrate for electrical isolation and mechanical support; a conducting "active" layer of width *h* whose conductance can be modulated by varying the 2-D charge density and drift velocity of carriers in the layer; "source" and "drain" electrodes that contact the active layer; a dielectric or depleted non-conducting layer of width *d* on top of the active layer; and a metallic gate electrode on top of this last layer. Like any transistor, the FET has three terminals, but the most common configuration for its use is as a circuit two-port, i.e., two of the electrodes (usually the source and gate) are connected together. In this configuration, the FET converts an input current-voltage (I-V) pair (gate voltage, gate current) into an output I-V pair (drain voltage, drain current). Hence, the modeler's task is to determine two equations for the output electrical quantities, referred to as "terminal relations."

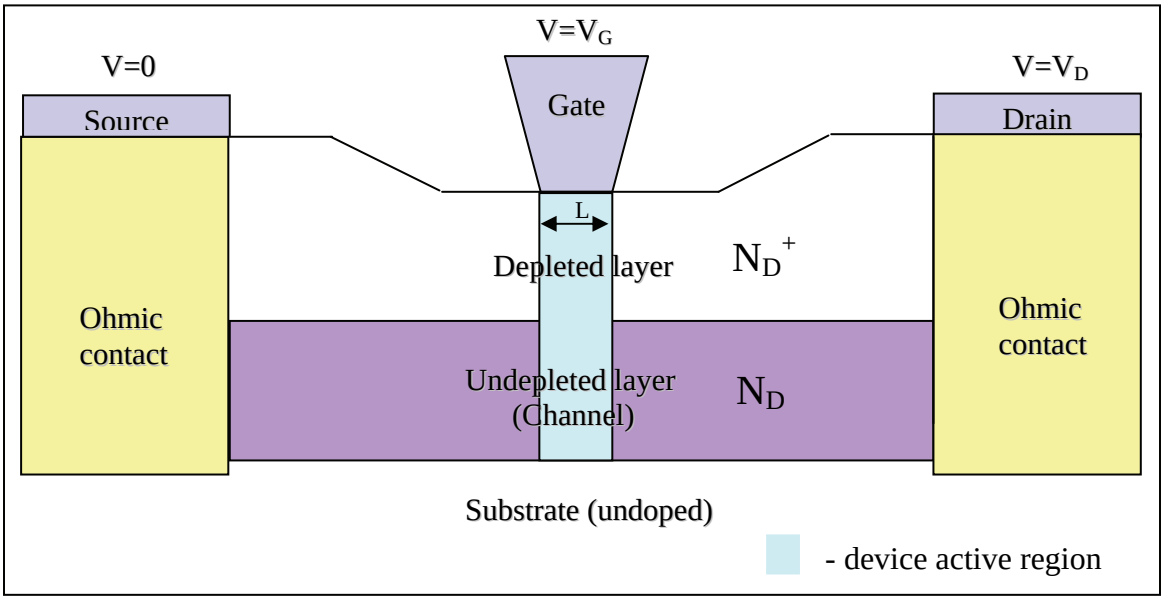

Figure 1. Typical FET geometry (gallium arsenide [GaAs] MESFET).

When voltages are applied to the electrodes, a highly non-uniform electric field exists inside the dielectric layer and a current flows within the active layer. The device operation is predicated on the degree of control each electrode voltage has over the electric field and current: the charge density in the channel is enhanced or suppressed by that "portion" of the electric field controlled by the gate electrode, while the drain electrode controls the carrier velocities through its "portion." While the concept of a "portion" is necessarily vague, it can be made more precise by introducing mutual capacitances (active and passive) between the electrodes. Because the electrodes are asymmetrically placed, it is expected that the current, like the field, is non-uniform. The distribution of potential within the structure is schematically shown in figure 2.

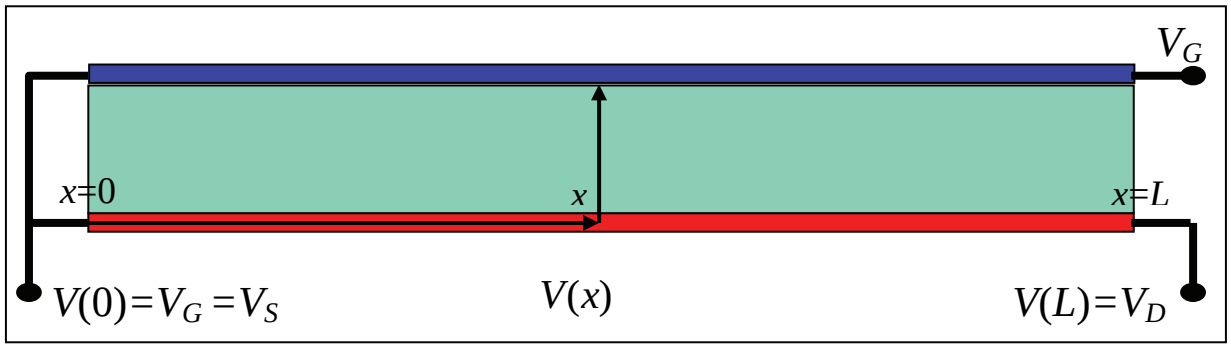

Figure 2. Relation between internal potential and terminal voltages. The red line indicates the FET channel, the blue line the gate.

In figure 2, $V(x)$ denotes the voltage at point x along the graphene layer and V_S, V_G, and V_D denote the voltages on the source, gate, and drain electrodes, respectively.

The guiding physical principle behind gradual-channel FET modeling is that the current flowing from source to drain be one-dimensional. Charge conservation then forces this current to be *uniform* everywhere. When this is so, the constant source-drain current I_D Is given by

$$I_D = ZhJ = Zqh\rho(V)\upsilon(E) \tag{1}$$

where Z is the width of the FET channel, h is its thickness, and the (fluid-mechanical) carrier current density $J = q\rho(V)\upsilon(E)$. In this expression, E is the electric field along the channel, q is the electron charge, $\upsilon(E)$ is the drift velocity of the carriers in the field E, $\rho(V)$ is the three-dimensional (3-D) number density (algebraic) of charge carriers in the channel, and V is the potential "associated" with E. For extremely thin channels, it is correct to introduce a 2-D density of charge carriers in the channel $n(V) = h\rho(V)$, so that the channel current of the FET is $I_D = Zq\upsilon(E)n(V)$.

It is clear that the field E and potential V are defined in a markedly inconsistent way. For the current to be constant, there must be no forces perpendicular to channel, implying that the field E must point *only* from source to drain inside the active layer. However, if this E is the gradient of

some potential *V*, the latter cannot depend on the voltage applied to the gate electrode, which contradicts the ability of the gate to control the channel charge. This difficulty is avoided in the gradual-channel model by assuming that the internal electric field changes direction abruptly at the boundary between the active layer and the dielectric/depleted layer. The interior field/current configuration is most easily represented by the circuit diagram shown in figure 3, which is that of a lossy and non-uniform transmission line.

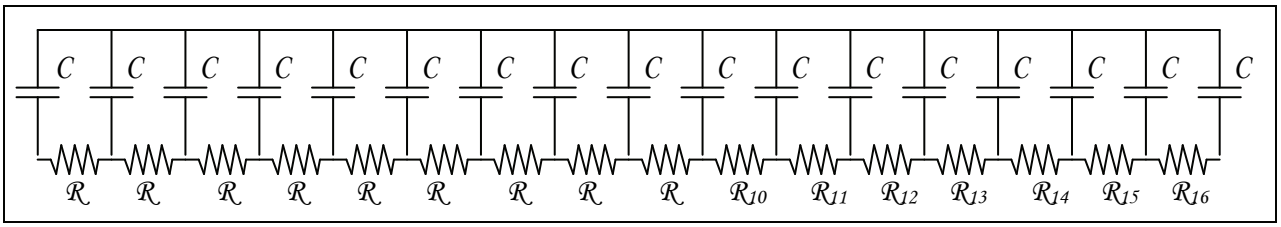

Figure 3. Lossy transmission line model of FET channel. Resistors $\mathcal{R}_I$ are functions of the local potential difference between channel and gate.

Although this picture of the internal electric field and carrier transport in a FET is fundamentally unrealistic, it has proved quite successful in reproducing the FET terminal characteristics, which points to considerable insensitivity of these characteristics to the detailed internal device dynamics. For this reason, most of the device models described in Sze's book on semiconductor devices (*4*) start with this model, which makes it an excellent template for comparing graphene devices with their better-known counterparts.

3. Modeling Methodology

Once the general concepts of the gradual-channel approach are accepted, the physics of the device operation are needed, that is, we must specify the functions $n(V)$ and $\upsilon(E)$. The former is derived primarily from the geometric structure of the device, the latter from microscopic features of the carrier transport.

3.1 Channel Carrier Density

Since *V* varies along the channel, modeling $n(V)$ involves the dielectric properties of the device interior. The capacitor-transmission line picture suggests that for a dielectric layer between gate and active layer,

$$\frac{q}{\varepsilon}n(V)=\frac{1}{d}\left(V_G-V_{th}\right)\Rightarrow n(V)=\frac{\varepsilon}{qd}\left(V_G-V_{th}\right) \tag{2}$$

where *d* is the dielectric layer thickness and V_{th} is a threshold voltage below which there are no carriers in the channel. In the MOSFET literature, this is simply known as the "linear model." Its use implies that the terminal characteristics exhibit no nonlinear behavior with drain voltage, and indeed the MOSFET at this level is simply a gate-controlled resistor. In an effort to explain current saturation in MOSFETs, Hofstein and Heiman (*5*) added a variation of $n(V)$ with the channel voltage *V*:

$$\frac{q}{\varepsilon}n(V)=\frac{1}{d}\left(V_G-V_{th}-V\right)\Rightarrow n(V)=\frac{\varepsilon}{qd}\left(V_G-V_{th}-V\right) \tag{3}$$

Within the gradual channel approximation this assumption leads to the I-V curve

$$I_D=\frac{Z\mu_0\varepsilon}{Ld}\left(\left[V_G-V_{th}\right]V_D-\frac{1}{2}{V_D}^2\right) \tag{4}$$

Here we note the appearance of a rather embarrassing feature of the gradual-channel model: for values of V_D greater than V_G-V_{th}, the current I_D decreases and eventually changes sign at $2\left(V_G-V_{th}\right)$. Because such a decrease in current with drain voltage under DC conditions is a sign of thermodynamic instability, its appearance here must be unphysical. It is tempting to assume that it arises solely from the poor description of the internal field in the gradual channel model, which should be fully 2-D, i.e., a solution of the 2-D Poisson equation; however, at least one of the many gradual channel models for MOSFETs—the Pao-Sah model (*6*)—avoids this problem completely without introducing 2-D effects. In this model, the functional form of $n(V)$ is quite complicated: for a *p* – MOSFET with semiconductor 3-D bulk charge densities p_{p0} (majority) and n_{p0} (minority),

$$\begin{aligned} n(V)&=\frac{1}{2}n_{p0}q^2\beta L_D\int_{\psi_s}^{\Phi}\frac{e^{\beta(\psi-V)}d\psi}{F(\beta\psi,\,V,\Delta)}\\ F(\beta\psi,\,V,\Delta)&=\left[e^{-\beta\psi}+\beta\psi+1+\Delta e^{-\beta V}\left(e^{\beta\psi}-\beta\psi e^{\beta V}-1\right)\right]^{1/2}\end{aligned} \tag{5}$$

where $\beta=\frac{1}{k_BT}$, $\Delta=\frac{n_{p0}}{p_{p0}}$, $L_D=\sqrt{\frac{2\varepsilon}{q\beta\sigma_b}}$ is the Debye length for the bulk material, $\sigma_b=p_{p0}$ is the majority-carrier bulk charge density, and ψ_s is the surface potential, which is evaluated from the gate voltage equation:

$$V_G - V_{FB} = \psi_S + \frac{2\varepsilon_S}{q\beta L_D}\left[e^{-\beta\psi_S} + \beta\psi_S + 1 + \Delta e^{-\beta V}\left(e^{\beta\psi_S} - \beta\psi_S e^{\beta V} - 1\right)\right]^{1/2} \quad (6)$$

Since its introduction in 1966, this model has regarded by designers of silicon-based device as too awkward and time-consuming to use. However, from the standpoint of designing graphene-based devices, its formulation includes two interesting features: in-channel ambipolarity, i.e., majority and minority carriers switch places within a pinched-off channel; and diffusion, which may be the key to its success in avoiding the need for fully 2-D computations. Unfortunately, the treatment of carriers in the channel is based on the Boltzmann equation for a gas of classical charged particles, which makes it unsuitable for the analysis of a truly 2-D channel, e.g., that of a HEMT.

3.2 Drift Velocity

At low electric fields, the drift velocity $\upsilon(E)$ of current carriers in a semiconductor can easily be derived from Ohm's law, i.e., $\upsilon(E) = \mu E$, where the mobility μ is taken to be a material constant. However, because most useful devices, including FETs, must operate under large-signal conditions, this linear result must be generalized to include large fields. One way to do this is to write $\upsilon(E) = \mu(E)E$, where $\mu(E)$ is derived from transport theory in bulk material. Because the derivation of $\mu(E)$ is a difficult problem even in this case, it is common practice to specify it empirically (*7*). From the standpoint of device design, the most important requirement for such an empirical description is that $\mu(E)$ incorporate the experimentally observed saturation of the carrier drift velocity $\upsilon(E)$ in most semiconductor materials. For graphene FETs, this exercise is highly useful. Several types of drift velocity relations are considered here, among them

3.2.1 The "Simulator" Model

$$\upsilon(E) = \frac{\mu_0 E}{1 + \dfrac{\mu_0 E}{\upsilon_{sat}}} \quad (7)$$

This expression (*7*) is commonly used for silicon (Si) devices and was in fact used recently by Meric et al. (*8*) to model graphene. In appendix A, it is shown that it leads to the I-V relation

$$I_D = \frac{\dfrac{Zq\mu_0}{L}\int_0^{V_D} n(V)\,dV}{1 + \dfrac{\mu_0}{L\upsilon_{sat}}\left|V_D\right|} \quad (8)$$

Using the MOSFET linear model for the channel, we can find the I-V relation explicitly.

$$\int_0^{V_D} n(V)\,dV = \frac{\varepsilon}{qd}\int_0^{V_D}\left(V_G - V\right)dV = \frac{\varepsilon}{qd}\left(V_G V_D - \frac{1}{2}{V_D}^2\right)$$

$$\Rightarrow I_D = \frac{\frac{Z\mu_0\varepsilon}{Ld}\left(V_G V_D - \frac{1}{2}{V_D}^2\right)}{1+\frac{\mu_0}{L\upsilon_{sat}}\left|V_D\right|} \tag{9}$$

Like the MOSFET model of Hofstein and Heiman, this model exhibits the problem that for values of V_D greater than V_G the current I_D decreases, and eventually changes sign at $2V_G$. This shows that the introduction of velocity saturation is not an automatic cure for the problem of thermodynamic instability.

The expression for $\mu(E)$ given previously is often used in numerical simulations, but its empirical nature suggests that is has very little physical content. Device models based on hot-electron transport, of which we will discuss two, are much more interesting:

3.2.2 Electron Heating Due to Phonons

The following velocity-field relation, which is derived from inelastic scattering by optical phonons in Conwell (*9*), is occasionally used in more detailed numerical simulations:

$$\upsilon(E) = \frac{\mu_0 E}{\sqrt{1+\left(\frac{\mu_0 E}{\upsilon_{sat}}\right)^2}} \tag{10}$$

A derivation of the I-V curve that corresponds to this expression is given in appendix A . This expression differs markedly from the “simulator” result:

$$I_D L = Zq\mu_0 \int_0^{V_D} \sqrt{n(V)^2 - \left[\frac{I_D}{Zq\upsilon_{sat}}\right]^2}\,dV \tag{11}$$

A related but slightly different velocity-field relation, derived from inelastic scattering by acoustic phonons:

$$\upsilon(E) = \frac{\mu_0 E}{\frac{1}{2} + \sqrt{\frac{1}{2} + \left(\frac{\mu_0 E}{\upsilon_{sat}}\right)^2}} \tag{12}$$

Despite the similarity of equations 11 and 12, the latter gives a rather strange result for the I-V curve:

$$I_D = \frac{1}{\frac{2\mu_0}{Zq\upsilon_{sat}^2}\int_0^{V_D}\frac{dV}{n(V)}}\left\{\sqrt{L^2 + 4\left(\frac{\mu_0}{\upsilon_{sat}}\right)^2\left[\int_0^{V_D}\frac{dV}{n(V)}\right]\left[\int_0^{V_D} n(V)\,dV\right]} - L\right\} \tag{13}$$

These two expressions will be discussed in a separate report.

4. Gradual-Channel Models for Graphene

With regard to device modeling in general, there are four peculiarities of graphene that distinguish it from bulk materials:

1. two-dimensionality
2. ambipolarity
3. zero band gap
4. a conical 2-D band structure

In this section of the report, I examine the impact of these features on three kinds of FET models, which differ in the way velocity saturation is modeled. My analysis focuses on the stability of the I-V curves (*10*), which is an important criterion for the usefulness of any FET model. I define a DC I-V curve as stable if it has no regions where drain current decreases with drain voltage. Stated another way, a stable DC I-V curve should exhibit no regions with negative AC output conductance. Since this parameter, along with the transconductance, are needed to specify the full low-frequency AC response of the FET and the AC equivalent circuit, stability of the I-V curve impacts predictions of microwave performance, i.e., the S-parameters of the device.

4.1 Modeling by Meric et al.

The first step to modeling a real FET structure is to incorporate a varying channel voltage into the expression for the channel charge density $n(V)$. In their paper (*8*), Meric et al. provide such an expression and use it in their initial effort to model the microwave response of a graphene FET. Because the authors wanted to study the role of ambipolarity in the functioning of their device, they equipped it with both a top and a back gate (figure 4), where the latter is used to "dope" the FET by electrostatically generating either *n*- or *p*-type graphene concentrations analogous to MOSFET channels. In what follows, I will discuss this FET model using data from their paper, denoting voltages on the top and back gates by V_{gst} and V_{gsb}, respectively.

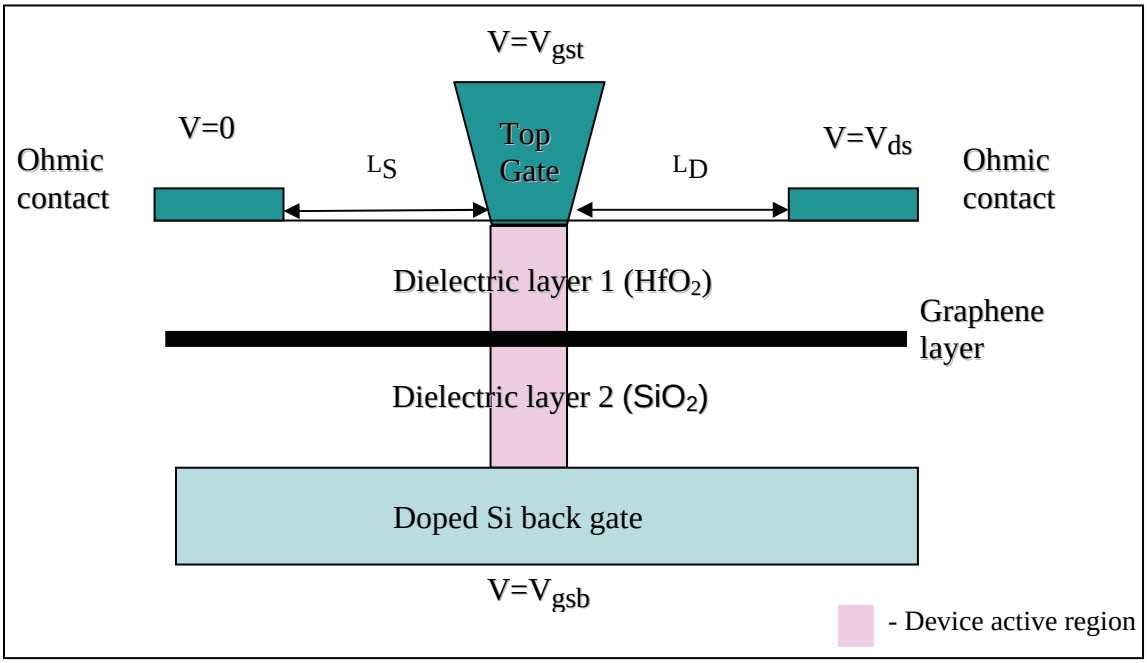

Figure 4. Dual-gate graphene FET structure of Meric et al.

In providing an expression for the channel carrier density $n(V)$, Meric et al. incorporate an additional peculiarity exhibited by graphene films: the existence of a "minimum conductivity" in the graphene channel, due apparently to ambipolarity. They do this by assuming that the minimum conductivity corresponds to a minimum carrier density n_0, and then using the following (empirical) expression for the function $n(V)$, which is now the total number of mobile carriers:

$$
\begin{aligned}
n(V) &= \sqrt{{n_0}^2 + \left(C_{gst}/q\right)^2 \left(V - V_{gst} - V_{th}\right)^2} \\
V_{th} &= {V_{gst}}^0 + \frac{C_{gsb}}{C_{gst}}\left(V_{gsb} - {V_{gsb}}^0\right)
\end{aligned}
\tag{14}
$$

The fact that this expression has a minimum at some voltage obscures the fact that neither the number of electrons nor the number of holes has such a minimum. It therefore sidesteps much of the discussion of ambipolar transport, but this is legitimate if electrons and holes have identical mobilities, which may be the case in graphene. The expression contains as fitting parameters two threshold gate voltages ${V_{gsb}}^0$, ${V_{gst}}^0$ at which the minimum carrier density n_0 is reached as the back and top gates are varied separately. The design numbers for this FET are

$$
\begin{aligned}
&Z = 2.1\ \mu\text{m} && C_{gst} = 552\ \text{nF/cm}^2 \\
&L = 1.0\ \mu\text{m} && {V_{gt}}^0 = 1.45\ \text{V} \\
&\mu_0 = 550\ \frac{\text{cm}^2}{\text{V}\cdot\text{s}} && C_{gsb} = 12\ \text{nF/cm}^2 \\
&\upsilon_F = 1.\times 10^8\ \text{cm/s} && {V_{gb}}^0 = 2.7\ \text{V} \\
&n_0 = 5\times 10^{11}\ \text{cm}^{-2}
\end{aligned}
\tag{15}
$$

where Z is the top gate width, L its length, μ_0 the channel mobility, υ_F the Fermi velocity for an infinite graphene sheet, n_0 the minimum channel density, C_{gst} the capacitance between the channel and top gate, and C_{gsb} the capacitance between the channel and back gate. Using these numbers and a back gate voltage of -40 V, they arrive at a threshold voltage for the channel of $V_{th} = 2.38$ V .

To model velocity saturation, they use the simulator expression, which leads to the following formula for I_D derived in appendix A:

$$
I_D = \frac{\dfrac{Zq\mu_0}{L}\displaystyle\int_0^{V_{ds}} n(V)\,dV}{1 + \dfrac{\mu_0}{L\upsilon_{sat}}\left|V_{ds}\right|}
\tag{16}
$$

Although they have written several papers relating to this modeling effort, Meric et al. are unclear as to the value of the saturation velocity υ_{sat}, although they mention the number 5.5×10^{7} cm/s (*8*). They justify their choice of the simulator expression (equation 16) implicitly by referencing to reference 7, but presumably simplicity was a factor as well. However, because this expression was developed for bulk-semiconductor devices, its use for graphene is open to criticism. One consequence of its use is the prediction of I-V curves that have a point of inflection, or "kink," when the biases drive the Dirac point into the channel. Their experimental curves do indeed show such a kink; however, the extent to which the latter can be explained by a gradual-channel model needs testing.

Because the expression for the I-V curves is explicit, it is easy to apply a stability test to it by computing the differential output conductance. From appendix B, we find that

$$\frac{dI_D}{dV_{ds}} = \frac{Zq\mu_0}{L}\left\{\begin{array}{l}\dfrac{\left(1+\dfrac{\mu_0}{L\upsilon_{sat}}V_{ds}\right)n\left(V_{ds}\right)-\dfrac{\mu_0}{L\upsilon_{sat}}\int_0^{V_{ds}} n(V)\,dV}{\left(1+\dfrac{\mu_0}{L\upsilon_{sat}}V_{ds}\right)^2}\Theta\left(V_{ds}\right) \\ +\dfrac{\left(1+\dfrac{\mu_0}{L\upsilon_{sat}}V_{ds}\right)n\left(V_{ds}\right)-\dfrac{\mu_0}{L\upsilon_{sat}}\int_0^{V_{ds}} n(V)\,dV}{\left(1+\dfrac{\mu_0}{L\upsilon_{sat}}V_{ds}\right)^2}\Theta\left(-V_{ds}\right)\end{array}\right\} \tag{17}$$

where I_D is given by equation 16. In appendix B, it is shown that the condition that this quantity always be positive is that

$$\begin{aligned} V_{ds} > 0 &\Rightarrow Zq\upsilon_{sat}\,n\left(V_{ds}\right) > I_D \\ V_{ds} < 0 &\Rightarrow Zq\upsilon_{sat}\,n\left(V_{ds}\right) > -I_D \end{aligned} \tag{18}$$

It is clear that if this inequality is violated, the violation will occur within a certain voltage interval $\left[V_-\,,\,V_+\right]$ bounded by points where $\left.\dfrac{dI_D}{dV_{ds}}\right|_{V_{ds}=V_\pm} = 0$, points that mark a peak and an adjacent trough in the S-shaped I-V curve. As the gate voltage is varied, this interval shrinks

to zero, at which point $V_- = V_+$. Denoting the common value of V_- and V_+ by V_c, we see that two equations

$$\left.\frac{dI_D}{dV_{ds}}\right|_{V_{ds}=V_c} = 0 \tag{19}$$

$$\left.\frac{d^2 I_D}{dV_{ds}^{\,2}}\right|_{V_{ds}=V_c} = 0 \tag{20}$$

are satisfied there simultaneously, so that the curve becomes almost flat. The second equation is the condition for a point of inflection in the I-V curve, i.e., a "kink." It should be emphasized that equation 19 and equation 18 can hold at the same time; indeed, these conditions are required for the presence of a physically acceptable kink. If $V_- \neq V_+$ there will be two points where $\frac{dI_D}{dV_{ds}} = 0$.

Let us demonstrate this for the expression used in reference 8. Since

$$n\left(V_{ds}\right) = n_0\sqrt{1+\left(\frac{C_{gst}}{n_0 q}\right)^2\left(V_{gst}-V_{ds}-V_{th}\right)^2}, \tag{21}$$

we find explicitly that

$$\int_0^{V_D} n(V)\,dV = \frac{n_0}{2\lambda}\left[\theta_{gs}-\theta_{gd}+\cosh\theta_{gs}\sinh\theta_{gs}-\cosh\theta_{gd}\sinh\theta_{gd}\right] \tag{22}$$

where $\lambda = \frac{C_{gst}}{n_0 q}$ and

$$\theta_{gd} = \sinh^{-1}\lambda\left(V_{gst}-V_{ds}-V_{th}\right) \qquad \theta_{gs} = \sinh^{-1}\lambda\left(V_{gst}-V_{th}\right) \tag{23}$$

Figure 5 shows plots of I_D versus V_{ds} and V_{gst} for three values of top-gate voltage for the transistor specified by the numbers given in reference 8 and listed above, along with a (rather low) value of 2.5×10^7 cm/s for υ_{sat}. For this transistor the threshold top-gate voltage for negative conductance is 3.58 V. The blue curves are below the threshold voltage for negative

conductance, and show a kink with positive slope; the red curves are for a device gated at threshold, where the kink has zero slope; and the yellow curves are for a device gated above threshold and have a region of negative conductance. The output conductance $s_d = \frac{dI_D}{dV_{ds}}$ and transconductance $g_m = \frac{dI_D}{dV_{gst}}$ are shown in figure 6; the absolute value of g_m is plotted in accordance with reference 8.

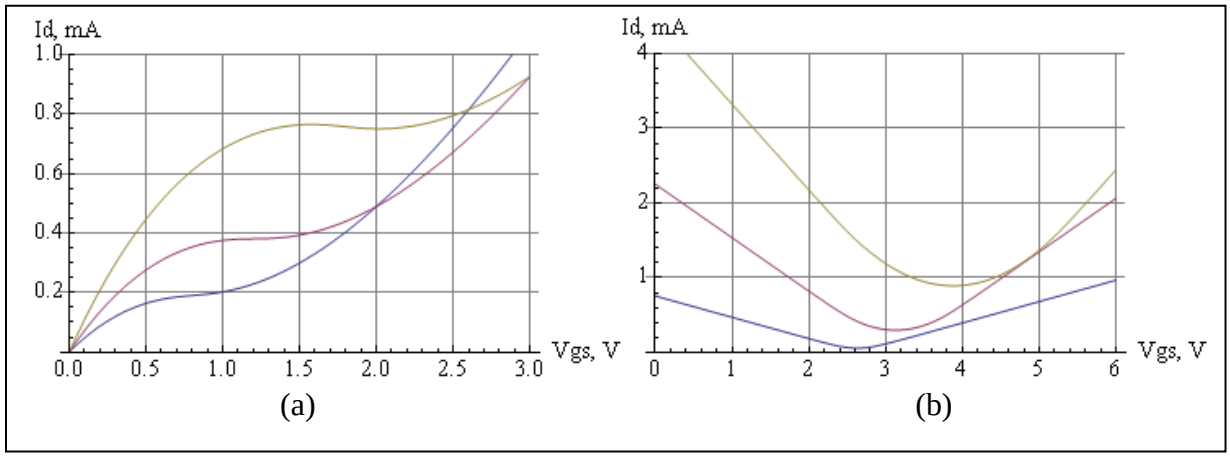

Figure 5. (a) I_D vs. V_{ds} for the simulator model and (b) I_D vs. V_{gst} for the simulator model.

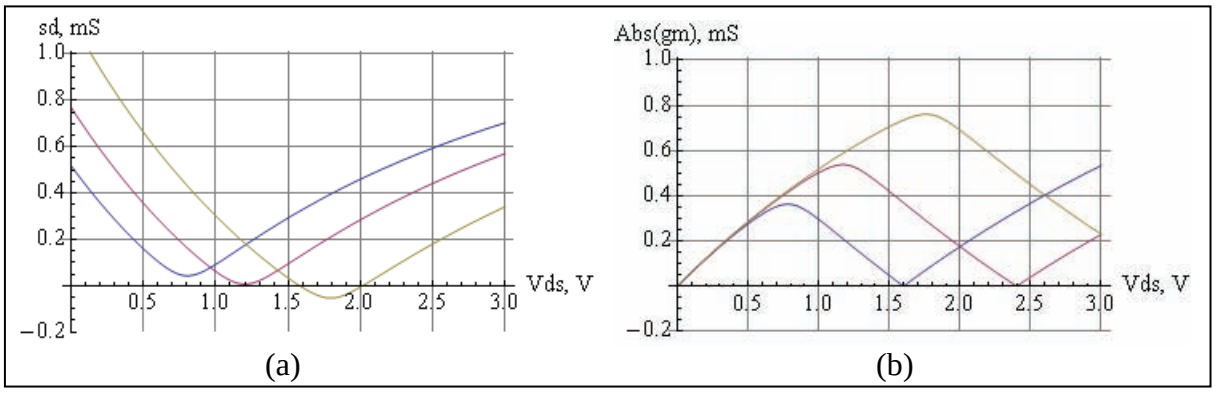

Figure 6. (a) s_d vs. V_{ds} for the simulator model and (b) $|g_m|$ vs. V_{ds} for the simulator model.

For the real devices Meric et al. investigated, it was necessary to include series "access" resistances associated with the source and drain contacts, leading to the following modified I-V expression (*11*):

$$I_D = \frac{\dfrac{Zq\mu_0}{L}\int_{R_s I_D}^{V_{ds}-R_s I_D} n(V)\,dV}{1+\dfrac{\mu_0}{L\upsilon_{sat}}\left|V_{ds}-2R_s I_D\right|} \tag{24}$$

which is now an implicit equation for the current. From appendix C, we find that

$$\frac{dI_D}{dV_{ds}} = \frac{\mu_0}{L\upsilon_{sat}}\left\{\begin{array}{l} \dfrac{Zq\upsilon_{sat}\,n\left(V_{ds}-R_s I_D\right)-I_D}{1+\dfrac{\mu_0}{L\upsilon_{sat}}\left(V_{ds}-4R_s I_D\right)+\dfrac{Zq\mu_0}{L}R_s\left[n\left(V_{ds}-R_s I_D\right)+n\left(R_s I_D\right)\right]}\Theta\left(V_{ds}-2R_s I_D\right) \\ +\dfrac{Zq\upsilon_{sat}\,n\left(V_{ds}-R_s I_D\right)+I_D}{1-\dfrac{\mu_0}{L\upsilon_{sat}}\left(V_{ds}-4R_s I_D\right)+\dfrac{Zq\mu_0}{L}R_s\left[n\left(V_{ds}-R_s I_D\right)+n\left(R_s I_D\right)\right]}\Theta\left(-V_{ds}+2R_s I_D\right) \end{array}\right\} \tag{25}$$

Then the condition that this quantity always be positive is that

$$\begin{aligned} V_{ds} > 2R_s I_D &\Rightarrow Zq\upsilon_{sat}\,n\left(V_{ds}-R_s I_D\right) > I_D \\ V_{ds} < 2R_s I_D &\Rightarrow Zq\upsilon_{sat}\,n\left(V_{ds}-R_s I_D\right) > -I_D \end{aligned} \tag{26}$$

which clearly reduces to equation 18 for no access resistances.

Using the expression introduced in reference 8:

$$n\left(V_{ds}-R_s I_D\right) = n_0\sqrt{1+\lambda^2\left(V_{gst}-V_{ds}-V_{th}+R_s I_D\right)^2}\,, \tag{27}$$

we again find explicitly that

$$\int_{R_s I_D}^{V_{ds}-R_s I_D} n(V)\,dV = \frac{1}{2\lambda} n_0 \left[\theta_{gss} - \theta_{gds} - \cosh\theta_{gds} \sinh\theta_{gds} + \cosh\theta_{gss} \sinh\theta_{gss} \right]$$

$$n\left(V_{ds} - R_s I_D\right) = n_0 \sqrt{1+\lambda^2 \left(V_{gst} - V_{ds} + R_s I_D - V_{th}\right)^2} = n_0 \cosh\theta_{gds} \qquad (28)$$

$$n\left(R_s I_D\right) = n_0 \sqrt{1+\lambda^2 \left(V_{gst} - R_s I_D - V_{th}\right)^2} = n_0 \cosh\theta_{gss}$$

and

$$\theta_{gds} = \sinh^{-1}\lambda\left(V_{gst} - V_{ds} + R_s I_D - V_{th}\right) \qquad \theta_{gss} = \sinh^{-1}\lambda\left(V_{gst} - R_s I_D - V_{th}\right) \qquad (29)$$

Figure 7 again shows plots of I_D versus V_{ds} and V_{gst} for the same three values of top-gate voltage, for the same transistor and numbers given above, with a value of 700 Ω for the access resistance R_s. Since the expression for I_D involves an implicit function for nonzero R_s, evaluation of I_D requires a numerical calculation; once it is computed, however, it can be inserted into the expressions for $\frac{dI_D}{dV_{ds}}$. The output conductance $s_d = \frac{dI_D}{dV_{ds}}$ and transconductance $g_m = \frac{dI_D}{dV_{gst}}$ are shown in figure 8.

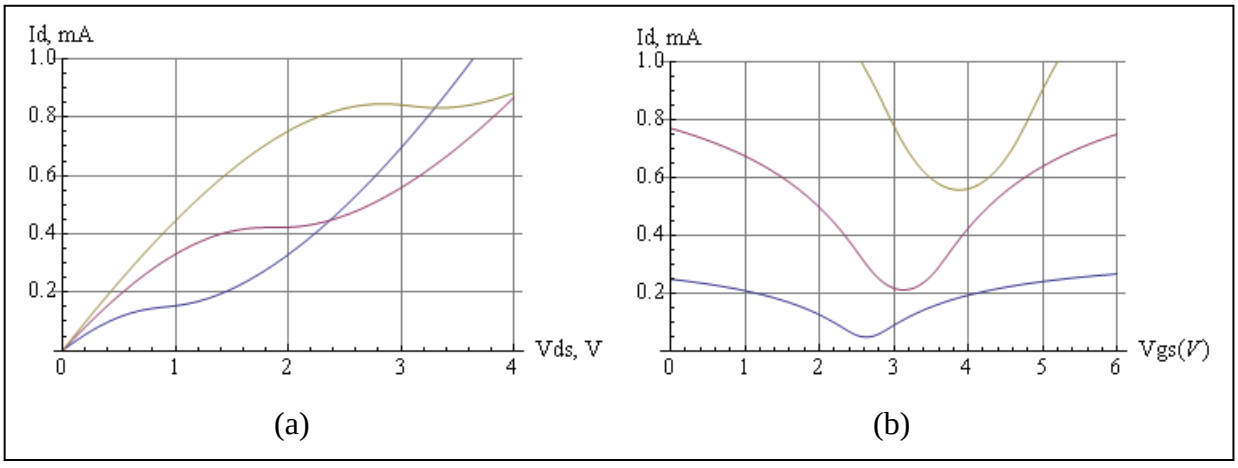

Figure 7. (a) I_D vs. V_{ds} for the simulator model with access resistances and (b) I_D vs. V_{gst} for the simulator model with access resistances.

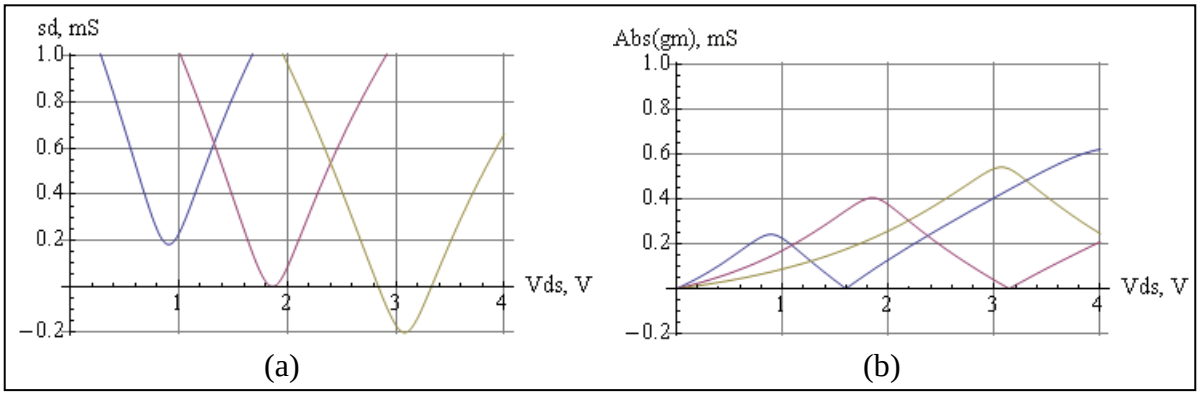

Figure 8. (a) s_d vs. V_{ds} for the simulator model and (b) $|g_m|$ vs. V_{ds} for the simulator model.

Let us compare the results of this calculation with the results for no access resistance. Note that the overall current output is suppressed, which is unsurprising; in addition, the conductance is much larger, a more obscure consequence of the additional 1400 Ω of access resistance. The threshold top gate voltage for kink formation is found to be 4.01 V, an increase over the value for no access resistance. Figure 8(b) shows curves similar to the experimental curves given in reference 12, including curvature to the left of the peak that is absent from the curves for transistors without access resistance.

4.2 Corrected Version of Simulator Model

The authors of reference 12 mention (and then seemingly discard) an interesting feature of carrier transport in graphene: the saturation velocity appears to be a function of carrier density, a phenomenon that has never been reported in ordinary FETs. To incorporate this effect, they make use of a semi-empirical dependence $\upsilon_{sat}(n) = \upsilon_F\left(\frac{\beta}{\sqrt{n}} - \alpha\right)$, where α and β are fitting parameters (α=0.07). The use of this function in simulations is problematic, since it allows υ_{sat} to become negative. The proper form of the I-V curve with this feature included is derived in appendix B, where we also replace the semi-empirical dependence with the following more reasonable approximation: since

$$\lim_{n\to 0}\frac{\beta}{\sqrt{n}+\frac{\alpha}{\beta}n} = \frac{\beta}{\sqrt{n}\left(1+\frac{\alpha}{\beta}\sqrt{n}\right)} \approx \frac{\beta}{\sqrt{n}}\left(1-\frac{\alpha}{\beta}\sqrt{n}\right) = \frac{\beta}{\sqrt{n}} - \alpha\,, \tag{30}$$

we can replace $\upsilon_{sat}(n) = \upsilon_F\left(\frac{\beta}{\sqrt{n}} - \alpha\right)$ by $\upsilon_{sat}(n) = \frac{\beta\upsilon_F}{\sqrt{n}\left(1+\frac{\alpha}{\beta}\sqrt{n}\right)}$ with little error. This procedure gives us a well-behaved dependence on *n* everywhere except at very low carrier densities.

The derivation given in appendix A is correct until we reach equation A-4. In order to include the density dependence of the saturation velocity, we need the expression

$$I_D = \frac{\frac{Zq\mu_0}{L}\int_0^{V_{ds}} n(V)dV}{1+\frac{\mu_0}{L}\left|\int_0^{V_{ds}} \frac{dV}{\upsilon_{sat}\left(n(V)\right)}\right|} \tag{31}$$

Using the "repaired" expression $\upsilon_{sat}(n) = \frac{\beta\upsilon_F}{\sqrt{n}\left(1+\frac{\alpha}{\beta}\sqrt{n}\right)}$ gives

$$I_D = \frac{\frac{Zq\mu_0}{L}H_1}{1+\frac{\mu_0}{\beta\upsilon_F L}\left|\frac{\alpha}{\beta}H_1 + H_2\right|} \tag{32}$$

where

$$H_1 = \int_0^{V_{ds}} n(V)\,dV \qquad H_2 = \int_0^{V_{ds}} \sqrt{n(V)}dV \tag{33}$$

Since $n(V) = n_0\sqrt{1+\lambda^2\left(V_{gst}-V-V_{th}\right)^2}$, we can evaluate these integrals. The first one was evaluated in the previous section:

$$\begin{aligned} H_1 &= \int_0^{V_{ds}} n(V)\,dV = n_0\int_0^{V_{ds}} \sqrt{1+\lambda^2\left(V_{gst}-V-V_{th}\right)^2}\,dV \\ &= \frac{1}{2}{n_0}^2\left(\frac{q}{C_{gst}}\right)\left[\theta_{gs}-\theta_{gd}+\cosh\theta_{gs}\sinh\theta_{gs}-\cosh\theta_{gd}\sinh\theta_{gd}\right] \end{aligned} \tag{34}$$

where $\theta_{gs} = \sinh^{-1}\lambda\left(V_{gst} - V_{th}\right)$, $\theta_{gd} = \sinh^{-1}\lambda\left(V_{gst} - V_{th} - V_{ds}\right)$. The second integral is more challenging, but it too can be evaluated in closed form:

$$H_2 = \int_0^{V_{ds}} \sqrt{n(V)}\,dV = n_0^{1/2} \int_0^{V_{ds}} \left[1+\lambda^2\left(V_{gst} - V_{th} - V\right)^2\right]^{1/4} dV$$
$$= \frac{1}{3} n_0^{3/2} \left(\frac{q}{C_{gst}}\right) \left[\begin{array}{l} \sinh\theta_{gs}\sqrt{\cosh\theta_{gs}} - \sinh\theta_{gd}\sqrt{\cosh\theta_{gd}} \\ +\frac{1}{\sqrt{2}}\,\mathrm{cn}^{-1}\left(\sqrt{\mathrm{sech}\theta_{gs}}\,|\,\frac{1}{2}\right) - \frac{1}{\sqrt{2}}\,\mathrm{cn}^{-1}\left(\sqrt{\mathrm{sech}\theta_{gd}}\,|\,\frac{1}{2}\right) \end{array}\right] \quad (35)$$

where $\mathrm{cn}^{-1}\left(x\,|\,\frac{1}{2}\right)$ is the inverse function of the Jacobi elliptic cosine $\mathrm{cn}\left(x\,|\,\frac{1}{2}\right)$.

For the stability check, we take the same derivative as before:

$$\frac{dI_D}{dV_{ds}} = \frac{Zq\mu_0}{L}\left[\frac{n\left(V_{ds}\right) - \frac{I_D}{Zq\beta\upsilon_F}\left\{\sqrt{n\left(V_{ds}\right)} + \frac{\alpha}{\beta}n\left(V_{ds}\right)\right\}}{1+\frac{\mu_0}{\beta\upsilon_F L}\left\{\frac{\alpha}{\beta}H_1 + H_2\right\}}\Theta\left(V_{ds}\right) + \frac{n\left(V_{ds}\right) + \frac{I_D}{Zq\beta\upsilon_F}\left\{\sqrt{n\left(V_{ds}\right)} + \frac{\alpha}{\beta}n\left(V_{ds}\right)\right\}}{1-\frac{\mu_0}{\beta\upsilon_F L}\left\{\frac{\alpha}{\beta}H_1 + H_2\right\}}\Theta\left(-V_{ds}\right)\right] \quad (36)$$

If we calculate the I-V curves of a graphene transistor using the parameters of Meric et al. and the corrected model, we get the curves shown in figure 9.

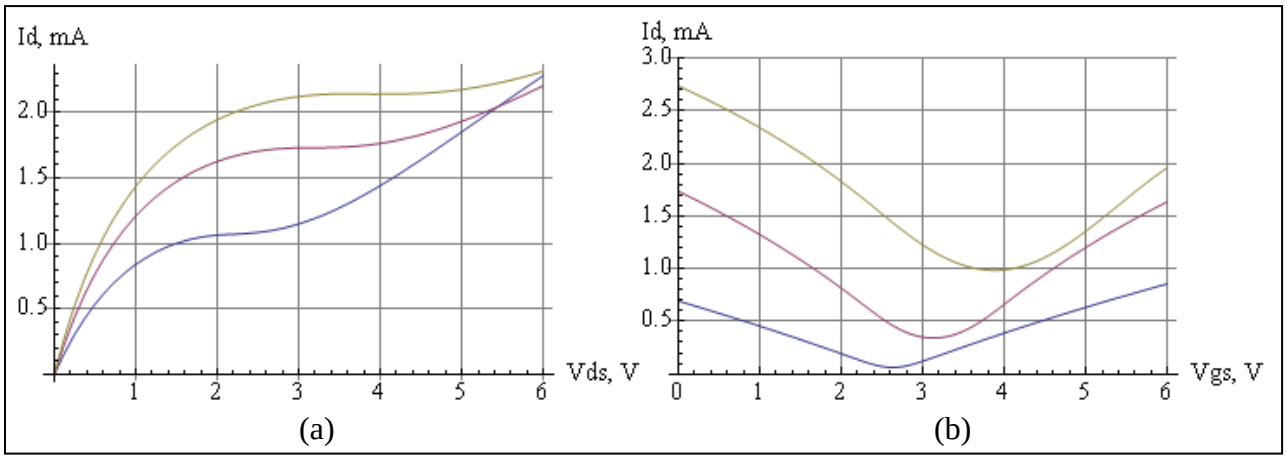

Figure 9. (a) I_D vs. V_{ds} in the corrected simulator model and (b) I_D vs. V_{gst} in the corrected simulator model.

We find that while a kink is still present, there is no trace of negative resistance in the voltage intervals shown. This feature of the corrected model is easier to see from a detailed comparison of the I-V curves shown in figures 10–16, where the corrected model predicts a lower current at a given voltage as the top-gate bias increases, with negligible negative-slope tendencies. Further computations indicate that the onset of an unphysical region in the I-V curve is postponed to a higher voltage (5.21 V) for the corrected model, but the actual negative slope is still extremely small for voltages as high as 7.58 V (figure 8a). This indicates that the corrected version is a more reliable guide to the transistor behavior over the range of drain and gate voltages of interest.

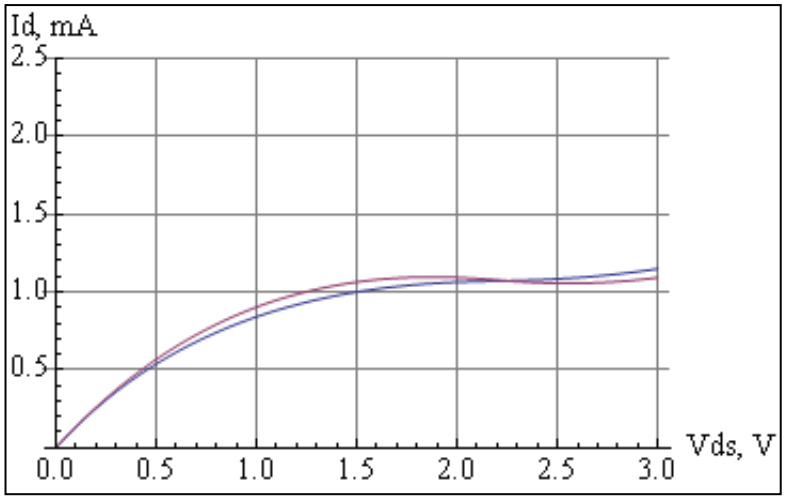

Figure 10. I_D vs. V_{ds} for V_{gst} = 3.18 V, blue curve-uncorrected model, red curve-corrected model.

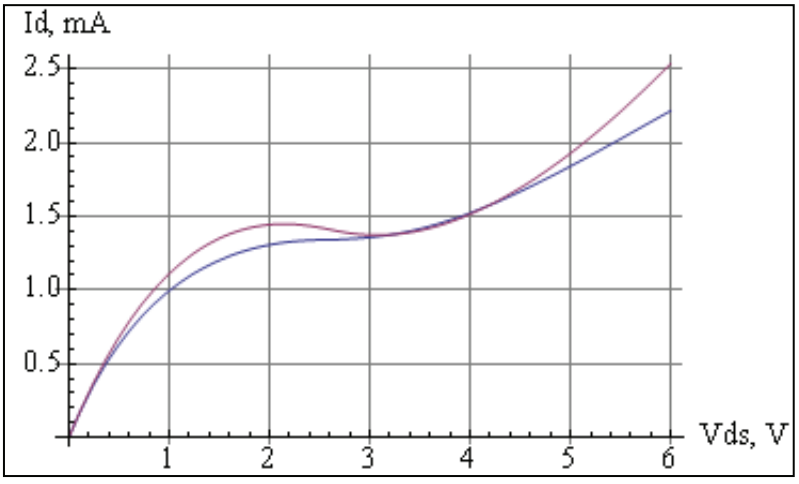

Figure 11. I_D vs. V_{ds} for V_{gst} = 3.58 V, blue curve-uncorrected model, red curve-corrected model.

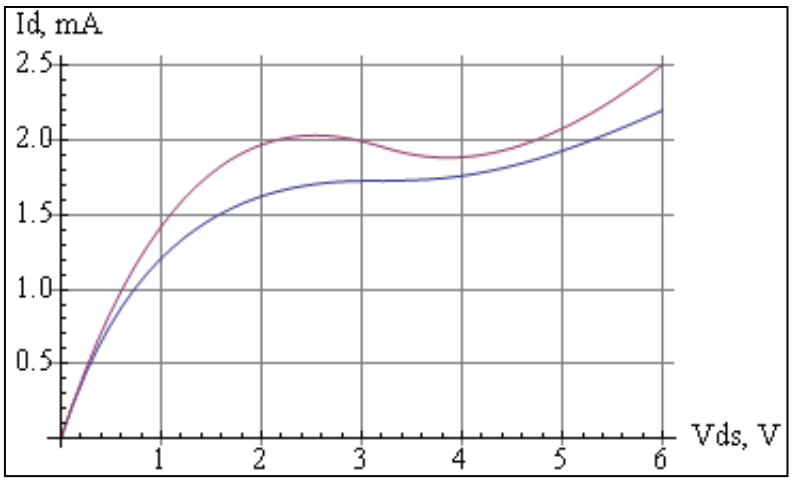

Figure 12. I_D vs. V_{ds} for V_{gst} = 4.18 V, blue curve-uncorrected model, red curve-corrected model

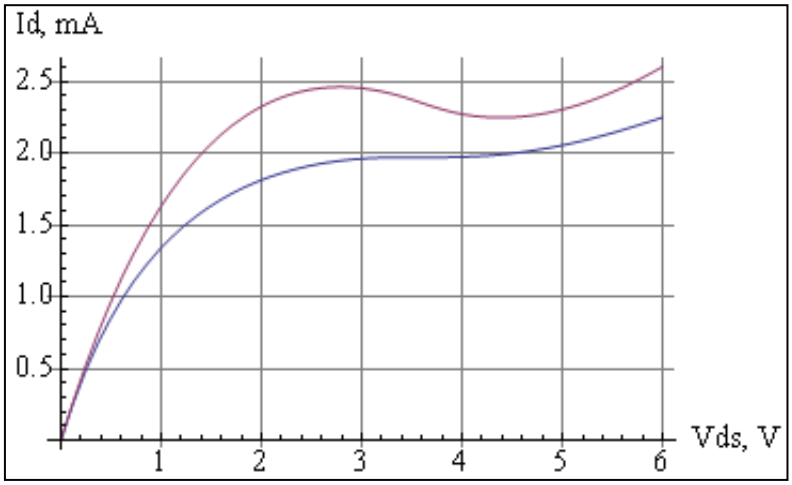

Figure 13. I_D vs. V_{ds} for V_{gst} = 4.58 V, blue curve-uncorrected model, red curve-corrected model.

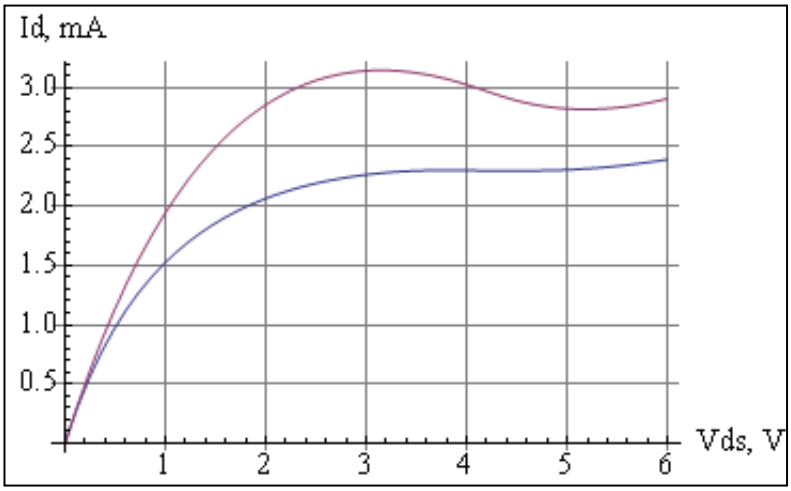

Figure 14. I_D vs. V_{ds} for V_{gst} = 5.18 V, blue curve-uncorrected model, red curve-corrected model.

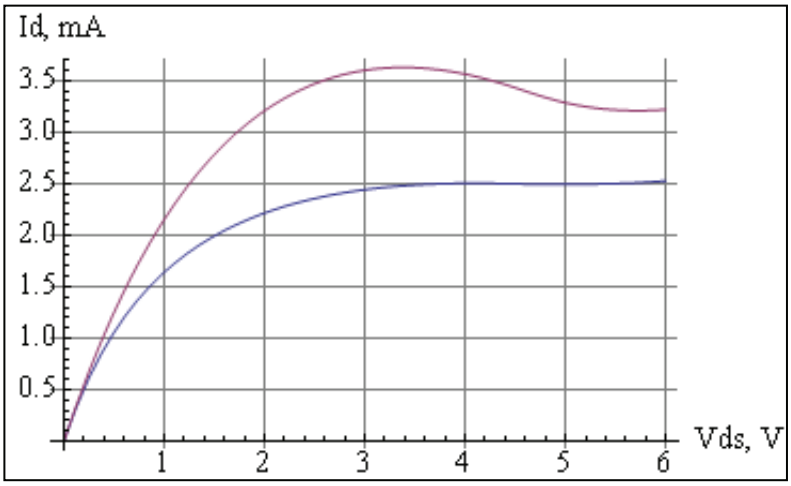

Figure 15. I_D vs. V_{ds} for V_{gst} = 5.58 V, blue curve-uncorrected model, red curve-corrected model.

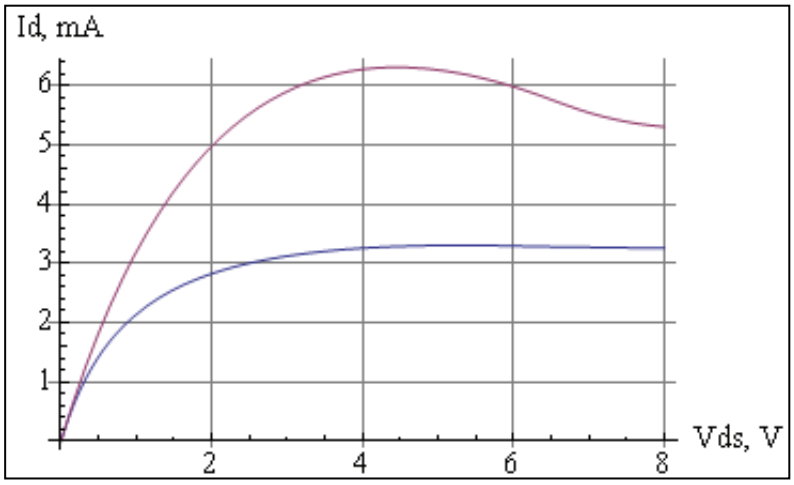

Figure 16. I_D vs. V_{ds} for V_{gst} = 7.58 V, blue curve-uncorrected model, red curve-corrected model.

Also of interest are the output conductance and transconductance predicted by the corrected model compared to those of the uncorrected model, which are shown in figures 17–22. For the transconductance the difference between the two models is not large, but the suppression of negative conductance is clearly seen in the output conductance for the corrected model. The more rapid decrease in the conductance away from the origin for the corrected model is also apparent.

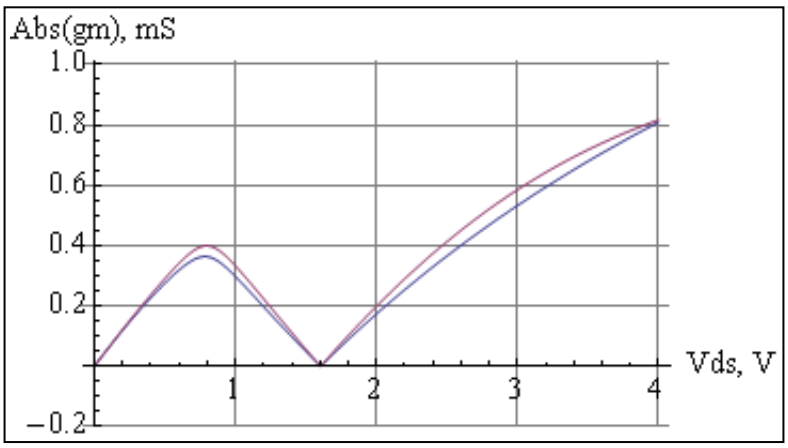

Figure 17. g_m vs. V_{ds} for V_{gst} = 3.18 V, blue curve-uncorrected model, red curve-corrected model.

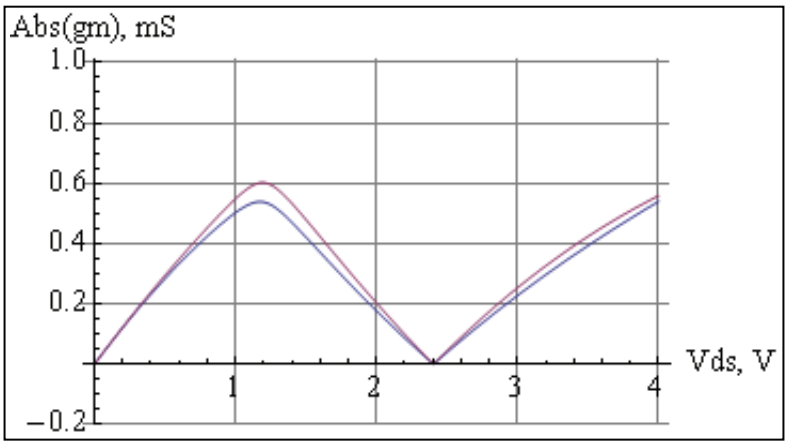

Figure 18. g_m vs. V_{ds} for V_{gst} = 3.58 V, blue curve-uncorrected model, red curve-corrected model.

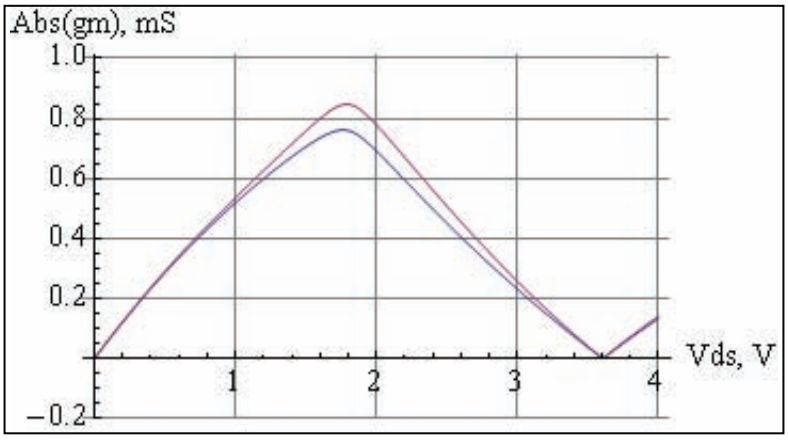

Figure 19. g_m vs. V_{ds} for V_{gst} = 4.18 V, blue curve-uncorrected model, red curve-corrected model.

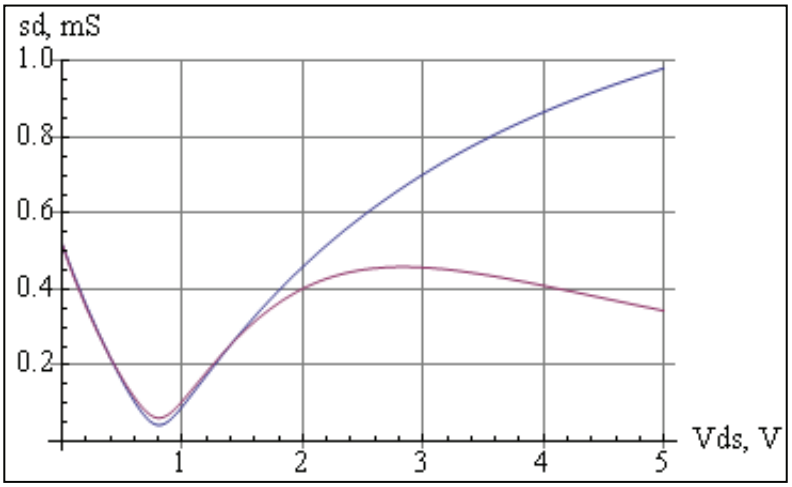

Figure 20. s_d vs. V_D for V_{gst} = 3.18 V, blue curve-uncorrected model, red curve-corrected model.

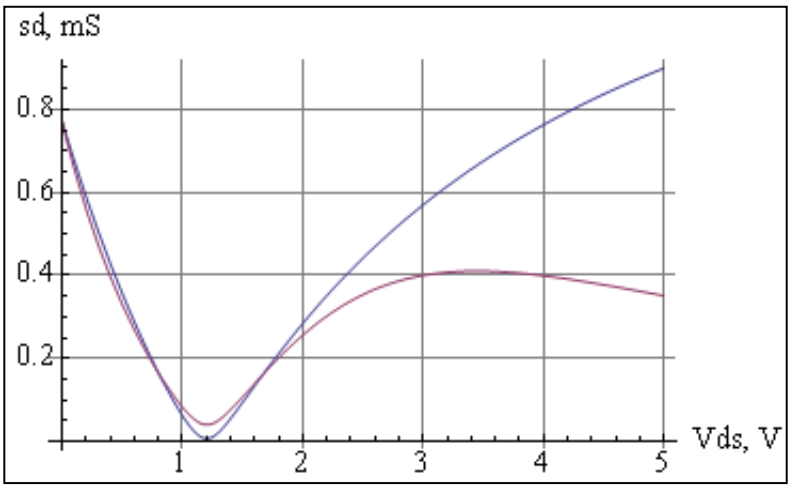

Figure 21. s_D vs. V_{ds} for V_{gst} = 3.58 V, blue curve-uncorrected model, red curve-corrected model.

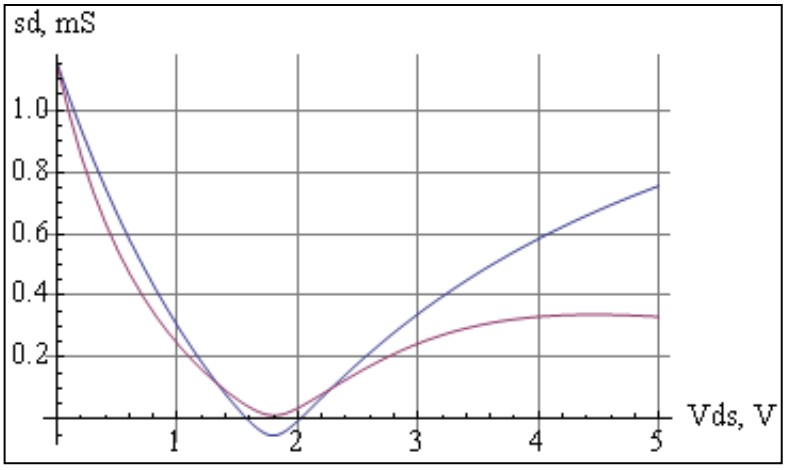

Figure 22. s_D vs. V_{ds} for V_{gst} = 4.18 V, blue curve-uncorrected model, red curve-corrected model.

5. Conclusions

It is interesting that the simulator model used by Meric et al. produces a negative resistance as soon as the channel current exceeds the maximum allowable current $Zq\upsilon_{sat}n\left(V_{ds}\right)$ at the drain end of the device. In standard two-region FET models, it is customary when this current is reached in part of the channel (the "saturated velocity region") to "pin" the variation of the channel density with respect to V_{ds} beyond this point. In such "two-region" models (*13*), increasing V_{ds} then increases the portion of the channel where the velocity is saturated, which increases the current slowly, and the device is defined to be "pinched off" once the entire channel is saturated and the current is a function only of the gate voltage. The saturation current that flows is referred to as I_{dss}. Two-region models do not exhibit negative resistance, but this is because of the ad-hoc division of the channel into segments.

Thanks to the papers by Meric et al., it is clear that simple modeling of the DC and microwave responses of graphene FETs is feasible. It is, however, important to choose a model that includes as many of the peculiarities of graphene as possible, in order to avoid a misleading picture of device function leading to false predictions and design errors. This report will be followed by a "physics-based" modeling effort, in which the model described here will be "fleshed out" with more realistic features.

7. References

1. See the bibliography of the article by Castro Neto, A. H.; Guinea, F.; Peres, N.M.R.; Novoselov, K. S.; Geim, A. K. The Electronic Properties of Graphene. *Reviews of Modern Physics* **2009**, *81*, 109.
2. Wallace, P. R. *Phys. Rev.* **1947**, *71*, 622.
3. Shockley, W. A Unipolar Field-effect Transistor. *Proc. IRE* **1952**, *40*, 1365–1376.
4. Sze, S. M. *Physics of Semiconductor Devices*; Wiley-Interscience, New York: Wiley, 1981, 2nd ed.
5. Hofstein, S. R.; Heiman, F. P. *Proc. IEEE* **1963**, *51*, 1190.
6. Pao, H. C.; Sah, C. T. *Solid-State Electronics* **1966**, *9*, 927; *IEEE Trans. Electron Devices* **1966**, *13*, 393.
7. Canali, C.; Majni, G.; Minder, R.; Ottaviani, G. *IEEE Trans. Electron Devices* **1975**, *ED-22*, 1045.
8. Meric, I.; Han, M.; Young, A. F.; Oyilmaz, B.; Kim, P.; Shepard, K. L. *Nature Nanotechnology (Letters)* **2008**, *3*, 654.
9. Cronwell, E. High Field Transport in Semiconductors, suppl. 9 in the series *Solid State Physics*, F. Seits, D. Turnbull, and H. Ehrenreich eds. (Academic Pres, New York, 1967).
10. Balkan, N.; Ridley, B. K.; Vickers, A. J. Negative Differential Resistance and Instabilities in 2-D Semiconductors, page 2, Springer, 1993.
11. Meric, I.; Han, M.; Young, A. F.; Ozyilmaz, B.; Kim, P.; Shepard, K. L. supplement to *Nature Nanotechnology (Letters)* **2008**, *3*, 654.
12. Meric, I.; Baklitskaya, N.; Kim, P.; Shepard, K. L. RF Performance of Top-gated, Zero-bandgap Graphene Field-effect Transistors. *2008 IEEE International Electron Devices Meeting* (IEEE, Piscataway, 2008), paper no. 4796738, pp. 1–4.
13. Pucel, R. A.; Haus, H. A.; Statz, H. Signal and Noise Properties of Gallium Arsenide Microwave Field-effect Transistors. *Adv. Electr. Electron. Phys.* **1974**, *38*, 195.

INTENTIONALLY LEFT BLANK.

Appendix A. Derivation of I-V Curves From Velocity-Field Relations

Three types of drift velocity relations are considered here

A-1 The "Simulator" Form

$$\upsilon(E) = \frac{\mu_0 E}{1 + \frac{\mu_0 |E|}{\upsilon_{sat}}}. \tag{A-1}$$

includes an absolute value function, which is an attempt to reflect the vector character of the drift velocity. In order to use this expression, we first write the local current in the channel at point *x* as

$$I_D(x) = Zq\upsilon\big(E(x)\big)n\big(V(x)\big) \tag{A-2}$$

Three electrical quantities – field, potential, and current – are connected by this expression, but a second relation is needed. To derive it, we first solve equation A-2 for *E*. The absolute value in the denominator makes this slightly tricky.

$$\begin{aligned} I_D &= Zq\frac{\mu_0 E}{1 + \frac{\mu_0 |E|}{\upsilon_{sat}}} n(V) \Rightarrow I_D\left(1 + \frac{\mu_0 |E|}{\upsilon_{sat}}\right) = Zq\mu_0 E\ n(V) \\ \Rightarrow Zq\mu_0 n(V)|E| &= |I_D|\left|1 + \frac{\mu_0 |E|}{\upsilon_{sat}}\right| = |I_D|\left(1 + \frac{\mu_0 |E|}{\upsilon_{sat}}\right) \end{aligned} \tag{A-3}$$

since the denominator in equation A-1 is always positive. Then

$$Zq\mu_0 n(V)|E| = |I_D| + |I_D|\frac{\mu_0|E|}{\upsilon_{sat}} \Rightarrow |E|\left(Zq\mu_0 n(V) - \frac{\mu_0|I_D|}{\upsilon_{sat}}\right) = |I_D|$$
$$\Rightarrow |E| = \frac{|I_D|}{Zq\mu_0 n(V) - \frac{\mu_0|I_D|}{\upsilon_{sat}}} \tag{A-4}$$

From this we get

$$1+\frac{\mu_0|E|}{\upsilon_{sat}} = 1+\frac{\frac{\mu_0}{\upsilon_{sat}}|I_D|}{Zq\mu_0 n(V) - \frac{\mu_0|I_D|}{\upsilon_{sat}}} = \frac{Zq\mu_0 n(V)}{Zq\mu_0 n(V) - \frac{\mu_0|I_D|}{\upsilon_{sat}}} \Rightarrow \frac{1}{1+\frac{\mu_0|E|}{\upsilon_{sat}}} = 1 - \frac{|I_D|}{Zqn(V)\upsilon_{sat}} \tag{A-5}$$

We now integrate equation A-1 over the distance x from source to drain, whose separation we call L:

$$\int_0^L I_D dx = Zq\int_0^L \frac{\mu_0 E}{1+\frac{\mu_0|E|}{\upsilon_{sat}}} n(V)dx = Zq\mu_0 \int_0^L \left(1 - \frac{|I_D|}{Zqn(V)\upsilon_{sat}}\right) n(V)Edx \tag{A-6}$$

But the constancy of I_D says that the left side of this equation is just $I_D L$. As for the right side, note that $E = \frac{dV}{dx} \Rightarrow Edx = dV$, so that

$$I_D L = Zq\mu_0 \int_0^{V_{ds}} \left(1 - \frac{|I_D|}{Zqn(V)\upsilon_{sat}}\right) n(V)dV$$
$$\Rightarrow I_D = \frac{Zq\mu_0}{L}\int_0^{V_{ds}} n(V)dV - \frac{\mu_0}{L}|I_D|\int_0^{V_{ds}} \frac{dV}{\upsilon_{sat}} \tag{A-7}$$

where V_{ds} is the source-drain voltage.

Let us label the two integrals $a = \frac{Zq\mu_0}{L}\int_0^{V_{ds}} n(V)dV$ and $b = \frac{\mu_0}{L}\int_0^{V_{ds}} \frac{dV}{\upsilon_{sat}}$, so that the equation to solve is

$$I_D = a - b|I_D| \tag{A-8}$$

The integrals *a* and *b* have positive integrands; hence, they have the same sign as the drain voltage V_{ds}. Figure A-1 shows plots of the functions $f\left(I_D\right) = I_D$ and $g\left(I_D\right) = a - b\left|I_D\right|$.

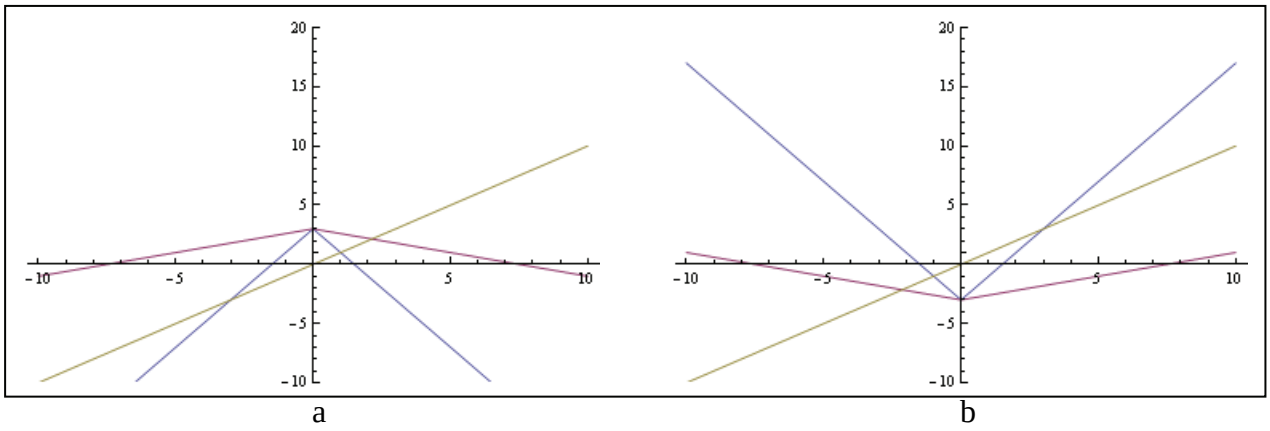

Figure A-1. Plots of the functions $f\left(x\right) = x$ and $g\left(x\right) = a - b\left|x\right|$ for (a) a = 3, b = 2 and a = 3, b = 0.4 and (b) a = –3, b = –2 and a = –3, b = –0.4.

For $V_{ds} > 0$ (figure A-1(*a*)) and $V_{ds} < 0$ (figure A-1b); the intersection of these functions defines the solutions to equation (A-3). It is clear from figure A-1a that equation A-8 always has a positive solution, and in addition a negative solution if $b > 1$; likewise, figure A-1b shows that equation A-8 always has a negative solution, plus a positive solution if $b > 1$. We reject the additional solutions as unphysical, in which case we easily find that

$$I_D = \begin{cases} \dfrac{a}{1+b} & V_{ds} > 0 \\ \dfrac{a}{1-b} & V_{ds} < 0 \end{cases} \Rightarrow I_D = \frac{a}{1+\left|b\right|} \tag{A-9}$$

and so the I-V curve is

$$I_D = \frac{\dfrac{Zq\mu_0}{L}\displaystyle\int_0^{V_{ds}} n\left(V\right)dV}{1+\left|\dfrac{\mu_0}{L}\displaystyle\int_0^{V_{ds}} \frac{dV}{\upsilon_{sat}}\right|} \tag{A-10}$$

In a bulk semiconductor the saturation velocity is a material quantity and therefore constant with voltage. Then it comes outside the integral, and so we have simply

$$I_D = \frac{\dfrac{Zq\mu_0}{L}\int_0^{V_{ds}} n(V)\,dV}{1+\dfrac{\mu_0}{L\upsilon_{sat}}\left|V_{ds}\right|} \tag{A-11}$$

where the nonanalyticity at $V_{ds} = 0$ is worth noting.

A-2 Hot-electron Physics of the Channel

Hot-electron physics of the channel leads to the following expression, associated with scattering by optical phonons:

$$\upsilon(E) = \frac{\mu_0 E}{\sqrt{1+\left(\dfrac{\mu_0 E}{\upsilon_{sat}}\right)^2}} \tag{A-12}$$

This resulting I-V curve differs markedly from the form derived in section A-1. Again we solve for *E*:

$$I_D{}^2 + I_D{}^2\left(\frac{\mu_0 E}{\upsilon_{sat}}\right)^2 = \left[Zq\mu_0 n(V)\right]^2 E^2 \Rightarrow E = \frac{I_D}{\sqrt{\left[Zq\mu_0 n(V)\right]^2 - \left[\mu_0 I_D/\upsilon_{sat}\right]^2}} \tag{A-13}$$

and as before,

$$\frac{1}{\sqrt{1+\left(\mu_0 E/\upsilon_{sat}\right)^2}} = \frac{1}{\sqrt{1+\dfrac{\left(\mu_0 I_D/\upsilon_{sat}\right)^2}{\left[Zq\mu_0 n(V)\right]^2 - \left[\mu_0 I_D/\upsilon_{sat}\right]^2}}} = \sqrt{1-\left[\frac{I_D}{Zqn(V)\upsilon_{sat}}\right]^2} \tag{A-14}$$

so that

$$I_D = \frac{Zq\mu_0}{L}\int_0^{V_{ds}} \sqrt{1-\left[\frac{I_D}{Zqn(V)\upsilon_{sat}}\right]^2}\, n(V)dV \tag{A-15}$$

A-3 Drift Velocity Associated with Acoustic Phonon Scattering

For the drift velocity associated with acoustic phonon scattering:

$$\upsilon(E) = \frac{\mu_0 E}{\frac{1}{2} + \sqrt{\frac{1}{2} + \left(\mu_0 E / \upsilon_{sat}\right)^2}} \tag{A-16}$$

solving for E gives

$$I_D = Zq\upsilon(E)n(V) = Zq\frac{\mu_0 E}{\frac{1}{2} + \sqrt{\frac{1}{4} + \left(\mu_0 E / \upsilon_{sat}\right)^2}} n(V)$$

$$\Rightarrow I_D \left\{1 + \sqrt{1 + \left(2\mu_0 E / \upsilon_{sat}\right)^2}\right\} = 2Zq\mu_0 En(V)$$

$$\Rightarrow {I_D}^2 + {I_D}^2 \left(2\mu_0 E / \upsilon_{sat}\right)^2 = \left(2Zq\mu_0 En(V) - I_D\right)^2$$

$$\Rightarrow {I_D}^2 \left(2\mu_0 E / \upsilon_{sat}\right)^2 E^2 = 4\left(Zq\mu_0 n(V)\right)^2 E^2 - 4Zq\mu_0 n(V) I_D E$$

$$\Rightarrow E = \frac{Zq\mu_0 n(V) I_D}{\left(Zq\mu_0 n(V)\right)^2 - \left(\mu_0 / \upsilon_{sat}\right)^2 {I_D}^2}$$

$$= \frac{1}{\mu_0} \frac{Zqn(V) I_D}{\left(Zqn(V)\right)^2 - \left(1/\upsilon_{sat}\right)^2 {I_D}^2} \Rightarrow \frac{\mu_0 E}{\upsilon_{sat}} = \frac{Zqn(V)\upsilon_{sat} I_D}{\left(Zqn(V)\upsilon_{sat}\right)^2 - {I_D}^2} \tag{A-17}$$

Setting $I_{sat} = Zqn(V)\upsilon_{sat}$, we find that

$$\frac{1}{2} + \sqrt{\frac{1}{4} + \left(\frac{\mu_0 E}{\upsilon_{sat}}\right)^2} = \frac{1}{2}\left\{1 + \sqrt{1 + \left(\frac{2I_{sat} I_D}{{I_{sat}}^2 - {I_D}^2}\right)^2}\right\}$$

$$1 + \left(\frac{2I_{sat} I_D}{{I_{sat}}^2 - {I_D}^2}\right)^2 = \frac{\left({I_{sat}}^2 - {I_D}^2\right)^2 + 4{I_{sat}}^2 {I_D}^2}{\left({I_{sat}}^2 - {I_D}^2\right)^2} = \left(\frac{{I_{sat}}^2 + {I_D}^2}{{I_{sat}}^2 - {I_D}^2}\right)^2 \tag{A-18}$$

$$\Rightarrow 1 + \sqrt{1 + \left(\frac{2I_{sat} I_D}{{I_{sat}}^2 - {I_D}^2}\right)^2} = 1 + \left|\frac{{I_{sat}}^2 + {I_D}^2}{{I_{sat}}^2 - {I_D}^2}\right|$$

Since ${I_{sat}}^2 > {I_D}^2$, we have

$$1+\sqrt{1+\left(\frac{2I_{sat}I_D}{{I_{sat}}^2-{I_D}^2}\right)^2}=1+\frac{{I_{sat}}^2+{I_D}^2}{{I_{sat}}^2-{I_D}^2}=\frac{2{I_{sat}}^2}{{I_{sat}}^2-{I_D}^2}$$

$$\Rightarrow\frac{1}{\frac{1}{2}+\sqrt{\frac{1}{4}+\left(\frac{\mu_0 E}{\upsilon_{sat}}\right)^2}}=\frac{2}{1+\sqrt{1+\left(\frac{2I_{sat}I_D}{{I_{sat}}^2-{I_D}^2}\right)^2}}=\frac{{I_{sat}}^2-{I_D}^2}{{I_{sat}}^2}=1-\frac{{I_D}^2}{{I_{sat}}^2} \qquad \text{(A-19)}$$

Then

$$I_D=Zq\frac{\mu_0 E}{\frac{1}{2}+\sqrt{\frac{1}{4}+\left(\mu_0 E/\upsilon_{sat}\right)^2}}n(V)\Rightarrow I_D L=Zq\mu_0\int_0^{V_{ds}}\frac{n(V)dV}{\frac{1}{2}+\sqrt{\frac{1}{4}+\left(\mu_0 E/\upsilon_{sat}\right)^2}}$$

$$=Zq\mu_0\int_0^{V_{ds}}n(V)\left[1-\frac{{I_D}^2}{{I_{sat}}^2}\right]dV=Zq\mu_0\int_0^{V_{ds}}n(V)dV-Zq\mu_0{I_D}^2\int_0^{V_{ds}}\frac{n(V)}{\left[Zqn(V)\upsilon_{sat}\right]^2}dV \qquad \text{(A-20)}$$

$$=Zq\mu_0\int_0^{V_{ds}}n(V)dV-\frac{\mu_0}{Zq{\upsilon_{sat}}^2}{I_D}^2\int_0^{V_{ds}}\frac{dV}{n(V)}\Rightarrow\left[\frac{\mu_0}{Zq{\upsilon_{sat}}^2}\int_0^{V_{ds}}\frac{dV}{n(V)}\right]{I_D}^2+I_D L=Zq\mu_0\int_0^{V_{ds}}n(V)dV$$

$$\Rightarrow I_D=\frac{1}{\frac{2\mu_0}{Zq{\upsilon_{sat}}^2}\int_0^{V_{ds}}\frac{dV}{n(V)}}\left\{\sqrt{L^2+4\left(\frac{\mu_0}{\upsilon_{sat}}\right)^2\left[\int_0^{V_{ds}}\frac{dV}{n(V)}\right]\left[\int_0^{V_{ds}}n(V)dV\right]}-L\right\}$$

Appendix B. Stability of Meric's I-V Curve Without Access Resistance

First, we calculate the output conductance:

$$I_D = \frac{\frac{Zq\mu_0}{L}\int_0^{V_{ds}} n(V)dV}{1+\frac{\mu_0}{L\upsilon_{sat}}\left|V_{ds}\right|} = \frac{\frac{Zq\mu_0}{L}\int_0^{V_{ds}} n(V)dV}{1+\frac{\mu_0}{L\upsilon_{sat}}V_{ds}}\Theta\left(V_{ds}\right) + \frac{\frac{Zq\mu_0}{L}\int_0^{V_{ds}} n(V)dV}{1-\frac{\mu_0}{L\upsilon_{sat}}V_{ds}}\Theta\left(-V_{ds}\right)$$

$$\frac{dI_D}{dV_{ds}} = \left\{\frac{d}{dV_{ds}}\frac{\frac{Zq\mu_0}{L}\int_0^{V_{ds}} n(V)dV}{1+\frac{\mu_0}{L\upsilon_{sat}}V_{ds}}\right\}\Theta\left(V_{ds}\right) + \left\{\frac{d}{dV_{ds}}\frac{\frac{Zq\mu_0}{L}\int_0^{V_{ds}} n(V)dV}{1-\frac{\mu_0}{L\upsilon_{sat}}V_{ds}}\right\}\Theta\left(-V_{ds}\right)$$

$$= \left\{\frac{d}{dV_{ds}}\frac{\frac{Zq\mu_0}{L}\int_0^{V_{ds}} n(V)dV}{1+\frac{\mu_0}{L\upsilon_{sat}}V_{ds}}\right\}\Theta\left(V_{ds}\right) + \left\{\frac{d}{dV_{ds}}\frac{\frac{Zq\mu_0}{L}\int_0^{V_{ds}} n(V)dV}{1-\frac{\mu_0}{L\upsilon_{sat}}V_{ds}}\right\}\Theta\left(-V_{ds}\right) \tag{B-1}$$

$$\frac{d}{dV_{ds}}\frac{\frac{Zq\mu_0}{L}\int_0^{V_{ds}} n(V)dV}{1\pm\frac{\mu_0}{L\upsilon_{sat}}V_{ds}} = \frac{\frac{Zq\mu_0}{L}n\left(V_{ds}\right)}{1\pm\frac{\mu_0}{L\upsilon_{sat}}V_{ds}} \mp \frac{\frac{\mu_0}{L\upsilon_{sat}}}{\left(1\pm\frac{\mu_0}{L\upsilon_{sat}}V_{ds}\right)^2}\frac{Zq\mu_0}{L}\int_0^{V_{ds}} n(V)dV$$

$$= \frac{Zq\mu_0}{L}\left\{\frac{\left(1\pm\frac{\mu_0}{L\upsilon_{sat}}V_{ds}\right)n\left(V_{ds}\right)\mp\frac{\mu_0}{L\upsilon_{sat}}\int_0^{V_{ds}} n(V)dV}{\left(1\pm\frac{\mu_0}{L\upsilon_{sat}}V_{ds}\right)^2}\right\} \tag{B-2}$$

$$\Rightarrow \frac{dI_D}{dV_{ds}} = \frac{Zq\mu_0}{L}\begin{cases} \dfrac{\left(1+\dfrac{\mu_0}{L\upsilon_{sat}}V_{ds}\right)n\left(V_{ds}\right)-\dfrac{\mu_0}{L\upsilon_{sat}}\int_0^{V_{ds}} n(V)\,dV}{\left(1+\dfrac{\mu_0}{L\upsilon_{sat}}V_{ds}\right)^2} & V_{ds}>0 \\ \dfrac{\left(1-\dfrac{\mu_0}{L\upsilon_{sat}}V_{ds}\right)n\left(V_{ds}\right)+\dfrac{\mu_0}{L\upsilon_{sat}}\int_0^{V_{ds}} n(V)\,dV}{\left(1-\dfrac{\mu_0}{L\upsilon_{sat}}V_{ds}\right)^2} & V_{ds}<0 \end{cases} \tag{B-3}$$

$$= \begin{cases} \dfrac{\dfrac{Zq\mu_0}{L}n\left(V_{ds}\right)-\dfrac{\mu_0}{L\upsilon_{sat}}I_D}{1+\dfrac{\mu_0}{L\upsilon_{sat}}V_{ds}} & V_{ds}>0 \\ \dfrac{\dfrac{Zq\mu_0}{L}n\left(V_{ds}\right)+\dfrac{\mu_0}{L\upsilon_{sat}}I_D}{1-\dfrac{\mu_0}{L\upsilon_{sat}}V_{ds}} & V_{ds}<0 \end{cases} = \frac{\mu_0}{L\upsilon_{sat}}\begin{cases} \dfrac{Zqn\left(V_{ds}\right)\upsilon_{sat}-I_D}{1+\dfrac{\mu_0}{L\upsilon_{sat}}V_{ds}} & V_{ds}>0 \\ \dfrac{Zqn\left(V_{ds}\right)\upsilon_{sat}+I_D}{1-\dfrac{\mu_0}{L\upsilon_{sat}}V_{ds}} & V_{ds}<0 \end{cases} \tag{B-4}$$

Then for $V_{ds}>0$ we get stability when

$$\frac{dI_D}{dV_{ds}} = \frac{Zq\mu_0}{L}\frac{\left(1+\dfrac{\mu_0}{L\upsilon_{sat}}V_{ds}\right)n\left(V_{ds}\right)-\dfrac{\mu_0}{L\upsilon_{sat}}\int_0^{V_{ds}} n(V)\,dV}{\left(1+\dfrac{\mu_0}{L\upsilon_{sat}}V_{ds}\right)^2} > 0$$

$$\Rightarrow Zq\upsilon_{sat}n\left(V_{ds}\right) > \frac{Zq\mu_0}{L}\frac{\int_0^{V_{ds}} n(V)\,dV}{1+\dfrac{\mu_0}{L\upsilon_{sat}}V_{ds}} = I_{ds} \tag{B-5}$$

while for $V_{ds}<0$ we have

$$\frac{dI_D}{dV_{ds}} = \frac{Zq\mu_0}{L} \frac{\left(1-\frac{\mu_0}{L\upsilon_{sat}}V_{ds}\right)n\left(V_{ds}\right)+\frac{\mu_0}{L\upsilon_{sat}}\int_0^{V_{ds}} n(V)\,dV}{\left(1-\frac{\mu_0}{L\upsilon_{sat}}V_{ds}\right)^2} > 0 \qquad \text{(B-6)}$$

$$\Rightarrow Zq\upsilon_{sat}n\left(V_{ds}\right) > -\frac{Zq\mu_0}{L}\frac{\int_0^{V_{ds}} n(V)\,dV}{1-\frac{\mu_0}{L\upsilon_{sat}}V_{ds}} = -I_{ds}$$

INTENTIONALLY LEFT BLANK.

Appendix C. Small-Signal Parameters From Meric's I-V Curve Without Access Resistance

C-1 Output Conductance

$$s_d = \frac{dI_D}{dV_{ds}} = \frac{\mu_0}{L\upsilon_{sat}} \begin{cases} \dfrac{Zqn\left(V_{ds}\right)\upsilon_{sat} - I_D}{1+\dfrac{\mu_0}{L\upsilon_{sat}}V_{ds}} & V_{ds} > 0 \\ \dfrac{Zqn\left(V_{ds}\right)\upsilon_{sat} + I_D}{1-\dfrac{\mu_0}{L\upsilon_{sat}}V_{ds}} & V_{ds} < 0 \end{cases} \tag{C-1}$$

C-2 Transconductance

In this section, we make the dependence of *n* on both gate and channel voltages explicit, i.e., we write $n(V)$ as $n\left(V,V_{gst}\right)$. Then

$$I_{ds} = \frac{\dfrac{Zq\mu_0}{L}\int_0^{V_{ds}} n\left(V,V_{gst}\right)dV}{1+\dfrac{\mu_0}{L\upsilon_{sat}}\left|V_{ds}\right|} \Rightarrow g_m = \frac{dI_{ds}}{dV_{gst}} = \frac{\dfrac{Zq\mu_0}{L}\int_0^{V_{ds}} \dfrac{d}{dV_{gt}} n\left(V,V_{gst}\right)dV}{1+\dfrac{\mu_0}{L\upsilon_{sat}}\left|V_{ds}\right|}$$

$$n\left(V,V_{gst}\right) = \sqrt{{n_0}^2 + \left(C_{gt}/q\right)^2\left(V - V_{gst} - V_{th}\right)^2} \Rightarrow \frac{d}{dV_{gt}} n\left(V,V_{gst}\right) = -\frac{d}{dV} n\left(V,V_{gst}\right)$$

$$\Rightarrow g_m = \frac{dI_D}{dV_{gst}} = -\frac{\dfrac{Zq\mu_0}{L}\int_0^{V_{ds}} \dfrac{d}{dV} n\left(V,V_{gst}\right)dV}{1+\dfrac{\mu_0}{L\upsilon_{sat}}\left|V_{ds}\right|} = -\frac{Zq\mu_0}{L}\left(\frac{n\left(V_{ds},V_{gst}\right) - n\left(0,V_{gst}\right)}{1+\dfrac{\mu_0}{L\upsilon_{sat}}\left|V_{ds}\right|}\right)$$

$$= \frac{Zq\mu_0}{L}\left(\frac{\sqrt{{n_0}^2 + \left(C_{gt}/q\right)^2 {V_{th}}^2} - \sqrt{{n_0}^2 + \left(C_{gt}/q\right)^2\left(V_{ds} - V_{gst} - V_{th}\right)^2}}{1+\dfrac{\mu_0}{L\upsilon_{sat}}\left|V_{ds}\right|}\right) \tag{C-2}$$

INTENTIONALLY LEFT BLANK.

Appendix D. Stability of Meric's I-V Curve With Access Resistance

Again, we calculate the output conductance:

$$I_D = \frac{\frac{Zq\mu_0}{L}\int_{R_s I_D}^{V_{ds}-R_s I_D} n(V)\,dV}{1+\frac{\mu_0}{L\upsilon_{sat}}\left|V_{ds}-2R_s I_D\right|} \tag{D-1}$$

$$= \frac{\frac{Zq\mu_0}{L}\int_{R_s I_D}^{V_{ds}-R_s I_D} n(V)\,dV}{1+\frac{\mu_0}{L\upsilon_{sat}}\left(V_{ds}-2R_s I_D\right)}\Theta\left(V_{ds}-2R_s I_D\right) + \frac{\frac{Zq\mu_0}{L}\int_{R_s I_D}^{V_{ds}-R_s I_D} n(V)\,dV}{1-\frac{\mu_0}{L\upsilon_{sat}}\left(V_{ds}-2R_s I_D\right)}\Theta\left(-V_{ds}+2R_s I_D\right)$$

$$V_{ds} > 2R_s I_D \Rightarrow \frac{dI_D}{dV_{ds}} = \frac{Zq\mu_0}{L}\frac{d}{dV_{ds}}\left\{\frac{\int_{R_s I_D}^{V_{ds}-R_s I_D} n(V)\,dV}{1+\frac{\mu_0}{L\upsilon_{sat}}\left(V_{ds}-2R_s I_D\right)}\right\}$$

$$= \frac{Zq\mu_0}{L}\left\{\frac{\frac{d}{dV_{ds}}\int_{R_s I_D}^{V_{ds}-R_s I_D} n(V)\,dV}{1+\frac{\mu_0}{L\upsilon_{sat}}\left(V_{ds}-2R_s I_D\right)} + \left(\int_{R_s I_D}^{V_{ds}-R_s I_D} n(V)\,dV\right)\frac{d}{dV_{ds}}\frac{1}{1+\frac{\mu_0}{L\upsilon_{sat}}\left(V_{ds}-2R_s I_D\right)}\right\} \tag{D-2}$$

$$\frac{d}{dV_{ds}}\int_{R_s I_D}^{V_{ds}-R_s I_D} n(V)\,dV = \frac{d}{dV_{ds}}\int_{0}^{V_{ds}-R_s I_D} n(V)\,dV - \frac{d}{dV_{ds}}\int_{0}^{R_s I_D} n(V)\,dV$$

$$\frac{d}{dV_{ds}}\int_{0}^{V_{ds}-R_sI_D} n(V)\,dV = \lim_{\Delta V_{ds}\to 0}\frac{1}{\Delta V_{ds}}\int_{V_{ds}-R_sI_D}^{V_{ds}-R_sI_D+\left(1-R_s\frac{dI_D}{dV_{ds}}\right)\Delta V_{ds}} n(V)\,dV$$

$$=\left(1-R_s\frac{dI_D}{dV_{ds}}\right)n\left(V_{ds}-R_sI_D\right)$$

$$\frac{d}{dV_{ds}}\int_{0}^{R_sI_D} n(V)\,dV = \frac{1}{\Delta V_{ds}}\int_{R_sI_D}^{R_sI_D+R_s\frac{dI_D}{dV_{ds}}\Delta V_{ds}} n(V)\,dV = R_s\frac{dI_D}{dV_{ds}}n\left(R_sI_D\right) \tag{D-3}$$

$$\Rightarrow \frac{d}{dV_{ds}}\int_{R_sI_D}^{V_{ds}-R_sI_D} n(V)\,dV = \left(1-R_s\frac{dI_D}{dV_{ds}}\right)n\left(V_{ds}-R_sI_D\right)-R_s\frac{dI_D}{dV_{ds}}n\left(R_sI_D\right)$$

$$=n\left(V_{ds}-R_sI_D\right)-R_s\left[n\left(V_{ds}-R_sI_D\right)+n\left(R_sI_D\right)\right]\frac{dI_D}{dV_{ds}}$$

$$\frac{d}{dV_{ds}}\frac{1}{1+\frac{\mu_0}{L\upsilon_{sat}}\left(V_{ds}-2R_sI_D\right)} = \frac{-1}{\left[1+\frac{\mu_0}{L\upsilon_{sat}}\left(V_{ds}-2R_sI_D\right)\right]^2}\frac{\mu_0}{L\upsilon_{sat}}\left(1-2R_s\frac{dI_D}{dV_{ds}}\right)$$

$$\Rightarrow \frac{dI_D}{dV_{ds}} = \frac{Zq\mu_0}{L}\left\{\begin{array}{l}\dfrac{n\left(V_{ds}-R_sI_D\right)-R_s\left[n\left(V_{ds}-R_sI_D\right)+n\left(R_sI_D\right)\right]\frac{dI_D}{dV_{ds}}}{1+\frac{\mu_0}{L\upsilon_{sat}}\left(V_{ds}-2R_sI_D\right)} \\ +\left(\int_{R_sI_D}^{V_{ds}-R_sI_D} n(V)\,dV\right)\dfrac{-1}{\left[1+\frac{\mu_0}{L\upsilon_{sat}}\left(V_{ds}-2R_sI_D\right)\right]^2}\dfrac{\mu_0}{L\upsilon_{sat}}\left(1-2R_s\dfrac{dI_D}{dV_{ds}}\right)\end{array}\right\} \tag{D-4}$$

$$= \frac{Zq\mu_0}{L}\left\{\frac{n\left(V_{ds}-R_sI_D\right)-R_s\left[n\left(V_{ds}-R_sI_D\right)+n\left(R_sI_D\right)\right]\frac{dI_D}{dV_{ds}}-\frac{L}{Zq\mu_0}I_D\frac{\mu_0}{L\upsilon_{sat}}\left(1-2R_s\frac{dI_D}{dV_{ds}}\right)}{1+\frac{\mu_0}{L\upsilon_{sat}}\left(V_{ds}-2R_sI_D\right)}\right\}$$

$$\Rightarrow\left[1+\frac{\mu_0}{L\upsilon_{sat}}\left(V_{ds}-2R_sI_D\right)\right]\frac{dI_D}{dV_{ds}}=\frac{Zq\mu_0}{L}\left\{\begin{array}{l} n\left(V_{ds}-R_sI_D\right)-\frac{L}{Zq\mu_0}I_D\frac{\mu_0}{L\upsilon_{sat}} \\ -R_s\left[n\left(V_{ds}-R_sI_D\right)+n\left(R_sI_D\right)\right]\frac{dI_D}{dV_{ds}} \\ +\frac{L}{Zq\mu_0}I_D\frac{\mu_0}{L\upsilon_{sat}}2R_s\frac{dI_D}{dV_{ds}}\end{array}\right\}$$

$$= \frac{Zq\mu_0}{L}\left\{n\left(V_{ds}-R_sI_D\right)-\frac{L}{Zq\mu_0}I_D\frac{\mu_0}{L\upsilon_{sat}}+\left(\frac{L}{Zq\mu_0}\frac{\mu_0}{L\upsilon_{sat}}2R_sI_D-R_s\left[n\left(V_{ds}-R_sI_D\right)+n\left(R_sI_D\right)\right]\right)\frac{dI_D}{dV_{ds}}\right\}$$

$$= \left\{\frac{Zq\mu_0}{L}n\left(V_{ds}-R_sI_D\right)-I_D\frac{\mu_0}{L\upsilon_{sat}}+\left(\frac{\mu_0}{L\upsilon_{sat}}2R_sI_D-\frac{Zq\mu_0}{L}R_s\left[n\left(V_{ds}-R_sI_D\right)+n\left(R_sI_D\right)\right]\right)\frac{dI_D}{dV_{ds}}\right\} \quad \text{(D-5)}$$

$$\Rightarrow\left[1+\frac{\mu_0}{L\upsilon_{sat}}\left(V_{ds}-2R_sI_D\right)-\left(\frac{\mu_0}{L\upsilon_{sat}}2R_sI_D-\frac{Zq\mu_0}{L}R_s\left[n\left(V_{ds}-R_sI_D\right)+n\left(R_sI_D\right)\right]\right)\right]\frac{dI_D}{dV_{ds}}$$

$$= \left\{\frac{Zq\mu_0}{L}n\left(V_{ds}-R_sI_D\right)-I_D\frac{\mu_0}{L\upsilon_{sat}}\right\} \quad \text{(D-6)}$$

$$\Rightarrow\left[\begin{array}{l}1+\frac{\mu_0}{L\upsilon_{sat}}\left(V_{ds}-4R_sI_D\right) \\ +\frac{Zq\mu_0}{L}R_s\left[n\left(V_{ds}-R_sI_D\right)+n\left(R_sI_D\right)\right]\end{array}\right]\frac{dI_D}{dV_{ds}}=\frac{Zq\mu_0}{L}n\left(V_{ds}-R_sI_D\right)-I_D\frac{\mu_0}{L\upsilon_{sat}}$$

$$\Rightarrow\frac{dI_D}{dV_{ds}}=\frac{\mu_0}{L\upsilon_{sat}}\frac{Zq\upsilon_{sat}n\left(V_{ds}-R_sI_D\right)-I_D}{1+\frac{\mu_0}{L\upsilon_{sat}}\left(V_{ds}-4R_sI_D\right)+\frac{Zq\mu_0}{L}R_s\left[n\left(V_{ds}-R_sI_D\right)+n\left(R_sI_D\right)\right]} \quad \text{(D-7)}$$

$$V_{ds} < 2R_s I_D \Rightarrow \frac{dI_D}{dV_{ds}} = \frac{Zq\mu_0}{L}\frac{d}{dV_{ds}}\left\{\frac{\int_{R_s I_D}^{V_{ds}-R_s I_D} n(V)\,dV}{1-\frac{\mu_0}{L\upsilon_{sat}}\left(V_{ds}-2R_s I_D\right)}\right\}$$

$$= \frac{Zq\mu_0}{L}\left\{\frac{\frac{d}{dV_{ds}}\int_{R_s I_D}^{V_{ds}-R_s I_D} n(V)\,dV}{1-\frac{\mu_0}{L\upsilon_{sat}}\left(V_{ds}-2R_s I_D\right)} + \left(\int_{R_s I_D}^{V_{ds}-R_s I_D} n(V)\,dV\right)\frac{d}{dV_{ds}}\frac{1}{1-\frac{\mu_0}{L\upsilon_{sat}}\left(V_{ds}-2R_s I_D\right)}\right\}$$

$$\frac{d}{dV_{ds}}\int_{R_s I_D}^{V_{ds}-R_s I_D} n(V)\,dV = n\left(V_{ds}-R_s I_D\right) - R_s\left[n\left(V_{ds}-R_s I_D\right)+n\left(R_s I_D\right)\right]\frac{dI_D}{dV_{ds}}$$

$$\frac{d}{dV_{ds}}\frac{1}{1-\frac{\mu_0}{L\upsilon_{sat}}\left(V_{ds}-2R_s I_D\right)} = \frac{-1}{\left[1-\frac{\mu_0}{L\upsilon_{sat}}\left(V_{ds}-2R_s I_D\right)\right]^2}\left(-\frac{\mu_0}{L\upsilon_{sat}}\right)\left(1-2R_s\frac{dI_D}{dV_{ds}}\right)$$

$$\Rightarrow \frac{dI_D}{dV_{ds}} = \frac{Zq\mu_0}{L}\left\{\begin{array}{l}\dfrac{n\left(V_{ds}-R_s I_D\right)-R_s\left[n\left(V_{ds}-R_s I_D\right)+n\left(R_s I_D\right)\right]\frac{dI_D}{dV_{ds}}}{1-\frac{\mu_0}{L\upsilon_{sat}}\left(V_{ds}-2R_s I_D\right)} \\ +\left(\int_{R_s I_D}^{V_{ds}-R_s I_D} n(V)\,dV\right)\dfrac{-1}{\left[1-\frac{\mu_0}{L\upsilon_{sat}}\left(V_{ds}-2R_s I_D\right)\right]^2}\left(-\frac{\mu_0}{L\upsilon_{sat}}\right)\left(1-2R_s\frac{dI_D}{dV_{ds}}\right)\end{array}\right\}$$

$$= \frac{Zq\mu_0}{L}\left\{\frac{n\left(V_{ds}-R_s I_D\right)-R_s\left[n\left(V_{ds}-R_s I_D\right)+n\left(R_s I_D\right)\right]\frac{dI_D}{dV_{ds}} + \frac{L}{Zq\mu_0}I_D\frac{\mu_0}{L\upsilon_{sat}}\left(1-2R_s\frac{dI_D}{dV_{ds}}\right)}{1-\frac{\mu_0}{L\upsilon_{sat}}\left(V_{ds}-2R_s I_D\right)}\right\} \quad \text{(D-8)}$$

$$\Rightarrow\left[1-\frac{\mu_0}{L\upsilon_{sat}}\left(V_{ds}-2R_sI_D\right)\right]\frac{dI_D}{dV_{ds}}=\frac{Zq\mu_0}{L}\left\{\begin{array}{l} n\left(V_{ds}-R_sI_D\right)+\frac{L}{Zq\mu_0}I_D\frac{\mu_0}{L\upsilon_{sat}} \\ -R_s\left[n\left(V_{ds}-R_sI_D\right)+n\left(R_sI_D\right)\right]\frac{dI_D}{dV_{ds}} \\ -\frac{L}{Zq\mu_0}I_D\frac{\mu_0}{L\upsilon_{sat}}2R_s\frac{dI_D}{dV_{ds}} \end{array}\right\} \quad \text{(D-9)}$$

$$=\frac{Zq\mu_0}{L}n\left(V_{ds}-R_sI_D\right)+I_D\frac{\mu_0}{L\upsilon_{sat}}-\left(\frac{\mu_0}{L\upsilon_{sat}}2R_sI_D+\frac{Zq\mu_0}{L}R_s\left[n\left(V_{ds}-R_sI_D\right)+n\left(R_sI_D\right)\right]\right)\frac{dI_D}{dV_{ds}}$$

$$\Rightarrow\left[1-\frac{\mu_0}{L\upsilon_{sat}}\left(V_{ds}-2R_sI_D\right)+\left(\frac{\mu_0}{L\upsilon_{sat}}2R_sI_D+\frac{Zq\mu_0}{L}R_s\left[n\left(V_{ds}-R_sI_D\right)+n\left(R_sI_D\right)\right]\right)\right]\frac{dI_D}{dV_{ds}}$$

$$=\left\{\frac{Zq\mu_0}{L}n\left(V_{ds}-R_sI_D\right)+I_D\frac{\mu_0}{L\upsilon_{sat}}\right\}$$

$$\Rightarrow\left[1-\frac{\mu_0}{L\upsilon_{sat}}\left(V_{ds}-4R_sI_D\right)+\frac{Zq\mu_0}{L}R_s\left[n\left(V_{ds}-R_sI_D\right)+n\left(R_sI_D\right)\right]\right]\frac{dI_D}{dV_{ds}}$$

$$=\left\{\frac{Zq\mu_0}{L}n\left(V_{ds}-R_sI_D\right)+I_D\frac{\mu_0}{L\upsilon_{sat}}\right\}$$

$$\Rightarrow\frac{dI_D}{dV_{ds}}=\frac{\mu_0}{L\upsilon_{sat}}\frac{Zq\upsilon_{sat}n\left(V_{ds}-R_sI_D\right)+I_D}{1-\frac{\mu_0}{L\upsilon_{sat}}\left(V_{ds}-4R_sI_D\right)+\frac{Zq\mu_0}{L}R_s\left[n\left(V_{ds}-R_sI_D\right)+n\left(R_sI_D\right)\right]} \quad \text{(D-10)}$$

Final Form:

$$\frac{dI_D}{dV_{ds}}=\frac{\mu_0}{L\upsilon_{sat}}\left\{\begin{array}{l} \frac{Zq\upsilon_{sat}n\left(V_{ds}-R_sI_D\right)-I_D}{1+\frac{\mu_0}{L\upsilon_{sat}}\left(V_{ds}-4R_sI_D\right)+\frac{Zq\mu_0}{L}R_s\left[n\left(V_{ds}-R_sI_D\right)+n\left(R_sI_D\right)\right]}\Theta\left(V_{ds}-2R_sI_D\right) \\ +\frac{Zq\upsilon_{sat}n\left(V_{ds}-R_sI_D\right)+I_D}{1-\frac{\mu_0}{L\upsilon_{sat}}\left(V_{ds}-4R_sI_D\right)+\frac{Zq\mu_0}{L}R_s\left[n\left(V_{ds}-R_sI_D\right)+n\left(R_sI_D\right)\right]}\Theta\left(-V_{ds}+2R_sI_D\right) \end{array}\right\} \quad \text{(D-11)}$$

INTENTIONALLY LEFT BLANK.

Appendix E. Small-Signal Parameters From Meric's I-V Curve With Access Resistance

E-1 Output Conductance

$$\frac{dI_D}{dV_{ds}} = \frac{\mu_0}{L\upsilon_{sat}}\left\{\begin{array}{l}\dfrac{Zq\upsilon_{sat}n\left(V_{ds}-R_sI_D\right)-I_D}{1+\dfrac{\mu_0}{L\upsilon_{sat}}\left(V_{ds}-4R_sI_D\right)+\dfrac{Zq\mu_0}{L}R_s\left[n\left(V_{ds}-R_sI_D\right)+n\left(R_sI_D\right)\right]}\Theta\left(V_{ds}-2R_sI_D\right) \\ +\dfrac{Zq\upsilon_{sat}n\left(V_{ds}-R_sI_D\right)+I_D}{1-\dfrac{\mu_0}{L\upsilon_{sat}}\left(V_{ds}-4R_sI_D\right)+\dfrac{Zq\mu_0}{L}R_s\left[n\left(V_{ds}-R_sI_D\right)+n\left(R_sI_D\right)\right]}\Theta\left(-V_{ds}+2R_sI_D\right)\end{array}\right\} \tag{E-1}$$

E-2 Transconductance

$$V_{ds} > 2R_sI_D \Rightarrow \frac{dI_D}{dV_{gst}} = \frac{Zq\mu_0}{L}\frac{d}{dV_{gst}}\left\{\frac{\int_{R_sI_D}^{V_{ds}-R_sI_D} n\left(V,V_{gst}\right)dV}{1+\dfrac{\mu_0}{L\upsilon_{sat}}\left(V_{ds}-2R_sI_D\right)}\right\} \tag{E-2}$$

$$= \frac{Zq\mu_0}{L}\left\{\frac{\dfrac{d}{dV_{gt}}\displaystyle\int_{R_sI_D}^{V_{ds}-R_sI_D} n\left(V,V_{gst}\right)dV}{1+\dfrac{\mu_0}{L\upsilon_{sat}}\left(V_{ds}-2R_sI_D\right)}+\left(\int_{R_sI_D}^{V_{ds}-R_sI_D} n\left(V,V_{gst}\right)dV\right)\frac{d}{dV_{gst}}\frac{1}{1+\dfrac{\mu_0}{L\upsilon_{sat}}\left(V_{ds}-2R_sI_D\right)}\right\}$$

$$\frac{d}{dV_{gst}}\int_{R_sI_D}^{V_{ds}-R_sI_D} n\left(V,V_{gst}\right)dV = \frac{d}{dV_{gst}}\int_{0}^{V_{ds}-R_sI_D} n\left(V,V_{gst}\right)dV - \frac{d}{dV_{gst}}\int_{0}^{R_sI_D} n\left(V,V_{gst}\right)dV$$

$$\frac{d}{dV_{gst}}\int_{0}^{V_{ds}-R_sI_D} n\left(V,V_{gst}\right)dV = \lim_{\Delta V_{gst}\to 0}\ \frac{1}{\Delta V_{gst}}\left\{\begin{array}{l}\displaystyle\int_{0}^{V_{ds}-R_s\left(I_D+\frac{dI_D}{dV_{gst}}\Delta V_{gst}\right)} n\left(V,V_{gst}+\Delta V_{gst}\right)dV \\ \displaystyle -\int_{0}^{V_{ds}-R_sI_D} n\left(V,V_{gst}\right)dV\end{array}\right\}$$

$$= \lim_{\Delta V_{gst}\to 0}\ \frac{1}{\Delta V_{gst}}\left\{\begin{array}{l}\displaystyle\int_{0}^{V_{ds}-R_s\left(I_D+\frac{dI_D}{dV_{gst}}\Delta V_{gst}\right)} \left[n\left(V,V_{gst}+\Delta V_{gst}\right)-n\left(V,V_{gst}\right)\right]dV \\ \displaystyle +\int_{V_{ds}-R_sI_D}^{V_{ds}-R_s\left(I_D+\frac{dI_D}{dV_{gst}}\Delta V_{gst}\right)} n\left(V,V_{gst}\right)dV\end{array}\right\}$$

$$= \int_{0}^{V_{ds}-R_sI_D}\frac{d}{dV_{gst}}n\left(V,V_{gst}\right)dV - R_s\frac{dI_D}{dV_{gst}}n\left(V_{ds}-R_sI_D,V_{gst}\right)$$

$$\frac{d}{dV_{gst}}\int_{0}^{R_sI_D} n\left(V,V_{gst}\right)dV = \int_{0}^{R_sI_D}\frac{d}{dV_{gst}}n\left(V,V_{gst}\right)dV + R_s\frac{dI_D}{dV_{gst}}n\left(R_sI_D,V_{gst}\right)$$

$$\Rightarrow \frac{d}{dV_{gst}}\int_{R_sI_D}^{V_{ds}-R_sI_D} n\left(V,V_{gst}\right)dV = \left\{\begin{array}{l}\displaystyle\int_{R_sI_D}^{V_{ds}-R_sI_D}\frac{d}{dV_{gst}}n\left(V,V_{gst}\right)dV \\ \displaystyle -R_s\frac{dI_D}{dV_{gst}}\left[n\left(V_{ds}-R_sI_D,V_{gst}\right)+n\left(R_sI_D,V_{gst}\right)\right]\end{array}\right\} \qquad \text{(E-3)}$$

$$\frac{d}{dV_{gst}}\frac{1}{1+\frac{\mu_0}{L\upsilon_{sat}}\left(V_{ds}-2R_sI_D\right)}=\frac{-1}{\left[1+\frac{\mu_0}{L\upsilon_{sat}}\left(V_{ds}-2R_sI_D\right)\right]^2}\left(-2R_s\frac{\mu_0}{L\upsilon_{sat}}\right)\frac{dI_D}{dV_{gst}}$$

$$\Rightarrow\frac{dI_D}{dV_{gst}}=\frac{Zq\mu_0}{L}\left\{\begin{array}{l}\dfrac{\int_{R_sI_D}^{V_{ds}-R_sI_D}\frac{d}{dV_{gst}}n\left(V,V_{gst}\right)dV-R_s\frac{dI_D}{dV_{gst}}\left[n\left(V_{ds}-R_sI_D,V_{gst}\right)+n\left(R_sI_D,V_{gst}\right)\right]}{1+\frac{\mu_0}{L\upsilon_{sat}}\left(V_{ds}-2R_sI_D\right)}\\ +\left(\int_{R_sI_D}^{V_{ds}-R_sI_D}n\left(V,V_{gst}\right)dV\right)\dfrac{2R_s\frac{\mu_0}{L\upsilon_{sat}}}{\left[1+\frac{\mu_0}{L\upsilon_{sat}}\left(V_{ds}-2R_sI_D\right)\right]^2}\frac{dI_D}{dV_{gst}}\end{array}\right\}$$

$$=\frac{Zq\mu_0}{L}\frac{\int_{R_sI_D}^{V_{ds}-R_sI_D}\frac{d}{dV_{gst}}n\left(V,V_{gst}\right)dV}{1+\frac{\mu_0}{L\upsilon_{sat}}\left(V_{ds}-2R_sI_D\right)}+\frac{2I_D\frac{\mu_0}{L\upsilon_{sat}}-\frac{Zq\mu_0}{L}\left[n\left(V_{ds}-R_sI_D,V_{gst}\right)+n\left(R_sI_D,V_{gst}\right)\right]}{1+\frac{\mu_0}{L\upsilon_{sat}}\left(V_{ds}-2R_sI_D\right)}R_s\frac{dI_D}{dV_{gst}} \quad \text{(E-4)}$$

$$\Rightarrow\left[1+\frac{\mu_0}{L\upsilon_{sat}}\left(V_{ds}-2R_sI_D\right)\right]\frac{dI_D}{dV_{gst}}=\frac{Zq\mu_0}{L}\int_{R_sI_D}^{V_{ds}-R_sI_D}\frac{d}{dV_{gst}}n\left(V,V_{gst}\right)dV$$

$$+\left\{2I_D\frac{\mu_0}{L\upsilon_{sat}}-\frac{Zq\mu_0}{L}\left[n\left(V_{ds}-R_sI_D,V_{gst}\right)+n\left(R_sI_D,V_{gst}\right)\right]\right\}R_s\frac{dI_D}{dV_{gst}}$$

$$\Rightarrow\left[1+\frac{\mu_0}{L\upsilon_{sat}}\left(V_{ds}-2R_sI_D\right)-2R_sI_D\frac{\mu_0}{L\upsilon_{sat}}+\frac{Zq\mu_0}{L}R_s\left[n\left(V_{ds}-R_sI_D,V_{gst}\right)+n\left(R_sI_D,V_{gst}\right)\right]\right]\frac{dI_D}{dV_{gst}}$$

$$=\frac{Zq\mu_0}{L}\int_{R_sI_D}^{V_{ds}-R_sI_D}\frac{d}{dV_{gst}}n\left(V,V_{gst}\right)dV$$

$$\Rightarrow\frac{dI_D}{dV_{gst}}=\frac{\frac{Zq\mu_0}{L}\int_{R_sI_D}^{V_{ds}-R_sI_D}\frac{d}{dV_{gst}}n\left(V,V_{gst}\right)dV}{1+\frac{\mu_0}{L\upsilon_{sat}}\left(V_{ds}-4R_sI_D\right)+\frac{Zq\mu_0}{L}R_s\left[n\left(V_{ds}-R_sI_D,V_{gst}\right)+n\left(R_sI_D,V_{gst}\right)\right]}$$

$$\Rightarrow g_m=-\frac{Zq\mu_0}{L}\frac{n\left(V_{ds}-R_sI_D,V_{gst}\right)-n\left(R_sI_D,V_{gst}\right)}{1+\frac{\mu_0}{L\upsilon_{sat}}\left(V_{ds}-4R_sI_D\right)+\frac{Zq\mu_0}{L}R_s\left[n\left(V_{ds}-R_sI_D,V_{gst}\right)+n\left(R_sI_D,V_{gst}\right)\right]} \quad \text{(E-5)}$$

$$V_{ds} < 2R_s I_D \Rightarrow \frac{dI_D}{dV_{gst}} = \frac{Zq\mu_0}{L}\frac{d}{dV_{gst}}\left\{\frac{\int_{R_s I_D}^{V_{ds}-R_s I_D} n\left(V,V_{gst}\right)dV}{1-\frac{\mu_0}{L\upsilon_{sat}}\left(V_{ds}-2R_s I_D\right)}\right\} \tag{E-6}$$

$$= \frac{Zq\mu_0}{L}\left\{\frac{\frac{d}{dV_{gst}}\int_{R_s I_D}^{V_{ds}-R_s I_D} n\left(V,V_{gst}\right)dV}{1-\frac{\mu_0}{L\upsilon_{sat}}\left(V_{ds}-2R_s I_D\right)} + \left(\int_{R_s I_D}^{V_{ds}-R_s I_D} n\left(V,V_{gst}\right)dV\right)\frac{d}{dV_{gst}}\frac{1}{1-\frac{\mu_0}{L\upsilon_{sat}}\left(V_{ds}-2R_s I_D\right)}\right\}$$

$$\frac{d}{dV_{gst}}\int_{R_s I_D}^{V_{ds}-R_s I_D} n\left(V,V_{gst}\right)dV = \int_{0}^{V_{ds}-R_s I_D}\frac{d}{dV_{gst}}n\left(V,V_{gst}\right)dV - R_s\frac{dI_D}{dV_{gst}}n\left(V_{ds}-R_s I_D,V_{gst}\right) \tag{E-7}$$

$$\frac{d}{dV_{gst}}\int_{0}^{R_s I_D} n\left(V,V_{gst}\right)dV = \int_{0}^{R_s I_D}\frac{d}{dV_{gst}}n\left(V,V_{gst}\right)dV + R_s\frac{dI_D}{dV_{gst}}n\left(R_s I_D,V_{gst}\right)$$

$$\Rightarrow \frac{d}{dV_{gst}}\int_{R_s I_D}^{V_{ds}-R_s I_D} n\left(V,V_{gst}\right)dV = \int_{R_s I_D}^{V_{ds}-R_s I_D}\frac{d}{dV_{gst}}n\left(V,V_{gst}\right)dV - R_s\frac{dI_D}{dV_{gst}}\left[n\left(V_{ds}-R_s I_D,V_{gst}\right)+n\left(R_s I_D,V_{gst}\right)\right]$$

$$\frac{d}{dV_{gst}}\frac{1}{1-\frac{\mu_0}{L\upsilon_{sat}}\left(V_{ds}-2R_s I_D\right)} = \frac{-1}{\left[1-\frac{\mu_0}{L\upsilon_{sat}}\left(V_{ds}-2R_s I_D\right)\right]^2}\left(+2R_s\frac{\mu_0}{L\upsilon_{sat}}\right)\frac{dI_D}{dV_{gst}}$$

$$\Rightarrow \frac{dI_D}{dV_{gst}} = \frac{Zq\mu_0}{L}\left\{\begin{array}{l}\dfrac{\int_{R_s I_D}^{V_{ds}-R_s I_D}\frac{d}{dV_{gst}}n\left(V,V_{gst}\right)dV - R_s\frac{dI_D}{dV_{gst}}\left[n\left(V_{ds}-R_s I_D,V_{gst}\right)+n\left(R_s I_D,V_{gst}\right)\right]}{1-\frac{\mu_0}{L\upsilon_{sat}}\left(V_{ds}-2R_s I_D\right)} \\ -\left(\int_{R_s I_D}^{V_{ds}-R_s I_D} n\left(V,V_{gst}\right)dV\right)\dfrac{2R_s\frac{\mu_0}{L\upsilon_{sat}}}{\left[1-\frac{\mu_0}{L\upsilon_{sat}}\left(V_{ds}-2R_s I_D\right)\right]^2}\frac{dI_D}{dV_{gst}}\end{array}\right\}$$

$$= \frac{Zq\mu_0}{L}\frac{\int_{R_s I_D}^{V_{ds}-R_s I_D}\frac{d}{dV_{gst}}n\left(V,V_{gst}\right)dV}{1-\frac{\mu_0}{L\upsilon_{sat}}\left(V_{ds}-2R_s I_D\right)} + \frac{-2I_D\frac{\mu_0}{L\upsilon_{sat}} - \frac{Zq\mu_0}{L}\left[n\left(V_{ds}-R_s I_D,V_{gst}\right)+n\left(R_s I_D,V_{gst}\right)\right]}{1-\frac{\mu_0}{L\upsilon_{sat}}\left(V_{ds}-2R_s I_D\right)}R_s\frac{dI_D}{dV_{gst}} \tag{E-8}$$

$$\Rightarrow\left[1-\frac{\mu_0}{L\upsilon_{sat}}\left(V_{ds}-2R_sI_D\right)\right]\frac{dI_D}{dV_{gst}}=\frac{Zq\mu_0}{L}\int_{R_sI_D}^{V_{ds}-R_sI_D}\frac{d}{dV_{gst}}n\left(V,V_{gst}\right)dV$$

$$+\left\{-2I_D\frac{\mu_0}{L\upsilon_{sat}}-\frac{Zq\mu_0}{L}\left[n\left(V_{ds}-R_sI_D,V_{gst}\right)+n\left(R_sI_D,V_{gst}\right)\right]\right\}R_s\frac{dI_D}{dV_{gst}}$$

$$\Rightarrow\left[1-\frac{\mu_0}{L\upsilon_{sat}}\left(V_{ds}-2R_sI_D\right)+2R_sI_D\frac{\mu_0}{L\upsilon_{sat}}+\frac{Zq\mu_0}{L}R_s\left[n\left(V_{ds}-R_sI_D,V_{gst}\right)+n\left(R_sI_D,V_{gst}\right)\right]\right]\frac{dI_D}{dV_{gst}}$$

$$=\frac{Zq\mu_0}{L}\int_{R_sI_D}^{V_{ds}-R_sI_D}\frac{d}{dV_{gst}}n\left(V,V_{gst}\right)dV$$

$$\Rightarrow\frac{dI_D}{dV_{gst}}=\frac{\frac{Zq\mu_0}{L}\int_{R_sI_D}^{V_{ds}-R_sI_D}\frac{d}{dV_{gst}}n\left(V,V_{gst}\right)dV}{1-\frac{\mu_0}{L\upsilon_{sat}}\left(V_{ds}-4R_sI_D\right)+\frac{Zq\mu_0}{L}R_s\left[n\left(V_{ds}-R_sI_D,V_{gst}\right)+n\left(R_sI_D,V_{gst}\right)\right]}$$

$$\Rightarrow g_m=-\frac{Zq\mu_0}{L}\frac{n\left(V_{ds}-R_sI_D,V_{gst}\right)-n\left(R_sI_D,V_{gst}\right)}{1-\frac{\mu_0}{L\upsilon_{sat}}\left(V_{ds}-4R_sI_D\right)+\frac{Zq\mu_0}{L}R_s\left[n\left(V_{ds}-R_sI_D,V_{gst}\right)+n\left(R_sI_D,V_{gst}\right)\right]} \quad \text{(E-9)}$$

Final form:

$$g_m=-\frac{Zq\mu_0}{L}\left\{\begin{array}{l}\dfrac{n\left(V_{ds}-R_sI_D,V_{gst}\right)-n\left(R_sI_D,V_{gst}\right)}{1+\frac{\mu_0}{L\upsilon_{sat}}\left(V_{ds}-4R_sI_D\right)+\frac{Zq\mu_0}{L}R_s\left[n\left(V_{ds}-R_sI_D,V_{gst}\right)+n\left(R_sI_D,V_{gst}\right)\right]}\Theta\left(V_{ds}-2R_sI_D\right)\\ -\dfrac{n\left(V_{ds}-R_sI_D,V_{gst}\right)-n\left(R_sI_D,V_{gst}\right)}{1-\frac{\mu_0}{L\upsilon_{sat}}\left(V_{ds}-4R_sI_D\right)+\frac{Zq\mu_0}{L}R_s\left[n\left(V_{ds}-R_sI_D,V_{gst}\right)+n\left(R_sI_D,V_{gst}\right)\right]}\Theta\left(-V_{ds}+2R_sI_D\right)\end{array}\right\} \quad \text{(E-10)}$$

INTENTIONALLY LEFT BLANK.

Appendix F. Modeling of Graphene FETS Using Meric et al. With Corrections (No Access Resistance)

The derivation used in appendix A is correct until we reach equation A-10. For tracking the density dependence of the saturation velocity, we need the following expression:

$$I_D = \frac{\frac{Zq\mu_0}{L}\int_0^{V_{ds}} n(V)dV}{1+\frac{\mu_0}{L}\left|\int_0^{V_{ds}} \frac{dV}{\upsilon_{sat}\left(n(V)\right)}\right|} \tag{F-1}$$

Using the "repaired" expression $\upsilon_{sat}(n) = \frac{\beta\upsilon_F}{\sqrt{n}\left(1+\frac{\alpha}{\beta}\sqrt{n}\right)}$ gives

$$I_D = \frac{\frac{Zq\mu_0}{L}\int_0^{V_{ds}} n(V)\,dV}{1+\frac{\mu_0}{\beta\upsilon_F L}\left|\int_0^{V_{ds}} \sqrt{n(V)}dV+\frac{\alpha}{\beta}\int_0^{V_{ds}} n(V)\,dV\right|} \equiv \frac{\frac{Zq\mu_0}{L}H_1}{1+\frac{\mu_0}{\beta\upsilon_F L}\left|H_2+\frac{\alpha}{\beta}H_1\right|} \tag{F-2}$$

$$\frac{dI_D}{dV_{ds}} = \frac{d}{dV_{ds}}\frac{\frac{Zq\mu_0}{L}\int_0^{V_{ds}} n(V)dV}{1+\frac{\mu_0}{\beta\upsilon_F L}\left|\int_0^{V_{ds}} \sqrt{n(V)}dV+\frac{\alpha}{\beta}\int_0^{V_{ds}} n(V)dV\right|} = \frac{d}{dV_{ds}}\left\{\begin{array}{l}\dfrac{\frac{Zq\mu_0}{L}\int_0^{V_{ds}} n(V)dV}{1+\frac{\mu_0}{\beta\upsilon_F L}\left\{\int_0^{V_{ds}} \sqrt{n(V)}dV+\frac{\alpha}{\beta}\int_0^{V_{ds}} n(V)dV\right\}}\Theta\left(V_{ds}\right) \\ +\dfrac{\frac{Zq\mu_0}{L}\int_0^{V_{ds}} n(V)dV}{1-\frac{\mu_0}{\beta\upsilon_F L}\left\{\int_0^{V_{ds}} \sqrt{n(V)}dV+\frac{\alpha}{\beta}\int_0^{V_{ds}} n(V)dV\right\}}\Theta\left(-V_{ds}\right)\end{array}\right\} \tag{F-3}$$

$$= \left\{ \begin{array}{l} \Theta\left(V_{ds}\right) \dfrac{d}{dV_{ds}} \dfrac{\dfrac{Zq\mu_0}{L} \int_0^{V_{ds}} n(V)\,dV}{1+\dfrac{\mu_0}{\beta \upsilon_F L}\left\{ \int_0^{V_{ds}} \sqrt{n(V)}\,dV + \dfrac{\alpha}{\beta} \int_0^{V_{ds}} n(V)\,dV \right\}} \\ +\Theta\left(-V_{ds}\right) \dfrac{d}{dV_{ds}} \dfrac{\dfrac{Zq\mu_0}{L} \int_0^{V_{ds}} n(V)\,dV}{1-\dfrac{\mu_0}{\beta \upsilon_F L}\left\{ \int_0^{V_{ds}} \sqrt{n(V)}\,dV + \dfrac{\alpha}{\beta} \int_0^{V_{ds}} n(V)\,dV \right\}} \end{array} \right\} \tag{F-4}$$

$$\frac{d}{dV_{ds}} \frac{\dfrac{Zq\mu_0}{L} \int_0^{V_{ds}} n(V)\,dV}{1+\dfrac{\mu_0}{\beta \upsilon_F L}\left\{ \int_0^{V_{ds}} \sqrt{n(V)}\,dV + \dfrac{\alpha}{\beta} \int_0^{V_{ds}} n(V)\,dV \right\}} = \frac{\dfrac{Zq\mu_0}{L} n\left(V_{ds}\right)}{1+\dfrac{\mu_0}{\beta \upsilon_F L}\left\{ \int_0^{V_{ds}} \sqrt{n(V)}\,dV + \dfrac{\alpha}{\beta} \int_0^{V_{ds}} n(V)\,dV \right\}}$$

$$+\frac{Zq\mu_0}{L} \int_0^{V_{ds}} n(V)\,dV \cdot \frac{(-1)\dfrac{\mu_0}{\beta \upsilon_F L} \dfrac{d}{dV_{ds}} \left\{ \int_0^{V_{ds}} \sqrt{n(V)}\,dV + \dfrac{\alpha}{\beta} \int_0^{V_{ds}} n(V)\,dV \right\}}{\left(1+\dfrac{\mu_0}{\beta \upsilon_F L}\left\{ \int_0^{V_{ds}} \sqrt{n(V)}\,dV + \dfrac{\alpha}{\beta} \int_0^{V_{ds}} n(V)\,dV \right\} \right)^2}$$

$$= \frac{Zq\mu_0}{L} \left\{ \begin{array}{l} \dfrac{n\left(V_{ds}\right)}{1+\dfrac{\mu_0}{\beta \upsilon_F L}\left\{ \int_0^{V_{ds}} \sqrt{n(V)}\,dV + \dfrac{\alpha}{\beta} \int_0^{V_{ds}} n(V)\,dV \right\}} - \dfrac{\mu_0}{\beta \upsilon_F L} H_1 \dfrac{\sqrt{n\left(V_{ds}\right)} + \dfrac{\alpha}{\beta} n\left(V_{ds}\right)}{\left(1+\dfrac{\mu_0}{\beta \upsilon_F L}\left\{ \int_0^{V_{ds}} \sqrt{n(V)}\,dV + \dfrac{\alpha}{\beta} \int_0^{V_{ds}} n(V)\,dV \right\} \right)^2} \end{array} \right\} \tag{F-5}$$

$$= \frac{Zq\mu_0}{L} \left\{ \begin{array}{l} \dfrac{n\left(V_{ds}\right)}{1+\dfrac{\mu_0}{\beta \upsilon_F L}\left\{ \dfrac{\alpha}{\beta} H_1 + H_2 \right\}} - \dfrac{\mu_0}{\beta \upsilon_F L} H_1 \dfrac{\sqrt{n\left(V_{ds}\right)} + \dfrac{\alpha}{\beta} n\left(V_{ds}\right)}{\left(1+\dfrac{\mu_0}{\beta \upsilon_F L}\left\{ \dfrac{\alpha}{\beta} H_1 + H_2 \right\} \right)^2} \end{array} \right\}$$

$$\frac{\frac{Zq\mu_0}{L}H_1}{1+\frac{\mu_0}{\beta\upsilon_F L}\left|H_2+\frac{\alpha}{\beta}H_1\right|}=I_D \Rightarrow \frac{Zq\mu_0}{L}\left\{\frac{n\left(V_{ds}\right)}{1+\frac{\mu_0}{\beta\upsilon_F L}\left\{\frac{\alpha}{\beta}H_1+H_2\right\}}-\frac{\mu_0}{\beta\upsilon_F L}H_1\frac{\sqrt{n\left(V_{ds}\right)}+\frac{\alpha}{\beta}n\left(V_{ds}\right)}{\left(1+\frac{\mu_0}{\beta\upsilon_F L}\left\{\frac{\alpha}{\beta}H_1+H_2\right\}\right)^2}\right\}$$

$$=\frac{Zq\mu_0}{L}\frac{n\left(V_{ds}\right)}{1+\frac{\mu_0}{\beta\upsilon_F L}\left\{\frac{\alpha}{\beta}H_1+H_2\right\}}-\frac{\mu_0}{\beta\upsilon_F L}\left(\frac{\sqrt{n\left(V_{ds}\right)}+\frac{\alpha}{\beta}n\left(V_{ds}\right)}{1+\frac{\mu_0}{\beta\upsilon_F L}\left\{\frac{\alpha}{\beta}H_1+H_2\right\}}\right)\frac{\frac{Zq\mu_0}{L}H_1}{1+\frac{\mu_0}{\beta\upsilon_F L}\left\{\frac{\alpha}{\beta}H_1+H_2\right\}}$$

$$=\frac{Zq\mu_0}{L}\frac{n\left(V_{ds}\right)}{1+\frac{\mu_0}{\beta\upsilon_F L}\left\{\frac{\alpha}{\beta}H_1+H_2\right\}}-\frac{\mu_0}{\beta\upsilon_F L}I_D\frac{\sqrt{n\left(V_{ds}\right)}+\frac{\alpha}{\beta}n\left(V_{ds}\right)}{1+\frac{\mu_0}{\beta\upsilon_F L}\left\{\frac{\alpha}{\beta}H_1+H_2\right\}}$$

$$=\frac{Zq\mu_0}{L}\left\{\frac{n\left(V_{ds}\right)-\frac{I_D}{Zq\beta\upsilon_F}\left\{\sqrt{n\left(V_{ds}\right)}+\frac{\alpha}{\beta}n\left(V_{ds}\right)\right\}}{1+\frac{\mu_0}{\beta\upsilon_F L}\left\{\frac{\alpha}{\beta}H_1+H_2\right\}}\right\} \qquad \text{(F-6)}$$

$$\Rightarrow \frac{d}{dV_{ds}}\frac{\frac{Zq\mu_0}{L}\int_0^{V_{ds}} n(V)\,dV}{1+\frac{\mu_0}{\beta\upsilon_F L}\left\{\int_0^{V_{ds}}\sqrt{n(V)}dV+\frac{\alpha}{\beta}\int_0^{V_{ds}} n(V)\,dV\right\}}=\frac{Zq\mu_0}{L}\left\{\frac{n\left(V_{ds}\right)-\frac{I_D}{Zq\beta\upsilon_F}\left\{\sqrt{n\left(V_{ds}\right)}+\frac{\alpha}{\beta}n\left(V_{ds}\right)\right\}}{1+\frac{\mu_0}{\beta\upsilon_F L}\left\{\frac{\alpha}{\beta}H_1+H_2\right\}}\right\}$$

$$\frac{d}{dV_{ds}}\frac{\frac{Zq\mu_0}{L}\int_0^{V_{ds}} n(V)dV}{1-\frac{\mu_0}{\beta\upsilon_F L}\left\{\int_0^{V_{ds}}\sqrt{n(V)}dV+\frac{\alpha}{\beta}\int_0^{V_{ds}} n(V)dV\right\}}=\frac{\frac{Zq\mu_0}{L}n\left(V_D\right)}{1-\frac{\mu_0}{\beta\upsilon_F L}\left\{\int_0^{V_{ds}}\sqrt{n(V)}dV+\frac{\alpha}{\beta}\int_0^{V_{ds}} n(V)dV\right\}}$$

$$+\frac{Zq\mu_0}{L}\int_0^{V_{ds}} n(V)dV\cdot\frac{(-1)\frac{\mu_0}{\beta\upsilon_F L}\frac{d}{dV_D}(-1)\left\{\int_0^{V_{ds}}\sqrt{n(V)}dV+\frac{\alpha}{\beta}\int_0^{V_{ds}} n(V)dV\right\}}{\left(1-\frac{\mu_0}{\beta\upsilon_F L}\left\{\int_0^{V_{ds}}\sqrt{n(V)}dV+\frac{\alpha}{\beta}\int_0^{V_{ds}} n(V)dV\right\}\right)^2}$$

$$=\frac{Zq\mu_0}{L}\left\{\frac{n\left(V_{ds}\right)}{1-\frac{\mu_0}{\beta\upsilon_F L}\left\{\int_0^{V_{ds}}\sqrt{n(V)}dV+\frac{\alpha}{\beta}\int_0^{V_{ds}} n(V)dV\right\}}+\frac{\mu_0}{\beta\upsilon_F L}H_1\frac{\sqrt{n\left(V_{ds}\right)}+\frac{\alpha}{\beta}n\left(V_{ds}\right)}{\left(1-\frac{\mu_0}{\beta\upsilon_F L}\left\{\int_0^{V_{ds}}\sqrt{n(V)}dV+\frac{\alpha}{\beta}\int_0^{V_{ds}} n(V)dV\right\}\right)^2}\right\} \quad \text{(F-7)}$$

$$=\frac{Zq\mu_0}{L}\left\{\frac{n\left(V_{ds}\right)}{1-\frac{\mu_0}{\beta\upsilon_F L}\left\{\frac{\alpha}{\beta}H_1+H_2\right\}}+\frac{\mu_0}{\beta\upsilon_F L}H_1\frac{\sqrt{n\left(V_{ds}\right)}+\frac{\alpha}{\beta}n\left(V_{ds}\right)}{\left(1-\frac{\mu_0}{\beta\upsilon_F L}\left\{\frac{\alpha}{\beta}H_1+H_2\right\}\right)^2}\right\}$$

$$\frac{\frac{Zq\mu_0}{L}H_1}{1-\frac{\mu_0}{\beta\upsilon_F L}\left|H_2+\frac{\alpha}{\beta}H_1\right|}=I_D \Rightarrow \frac{Zq\mu_0}{L}\left\{\frac{n\left(V_{ds}\right)}{1-\frac{\mu_0}{\beta\upsilon_F L}\left\{\frac{\alpha}{\beta}H_1+H_2\right\}}+\frac{\mu_0}{\beta\upsilon_F L}H_1\frac{\sqrt{n\left(V_{ds}\right)}+\frac{\alpha}{\beta}n\left(V_{ds}\right)}{\left(1-\frac{\mu_0}{\beta\upsilon_F L}\left\{\frac{\alpha}{\beta}H_1+H_2\right\}\right)^2}\right\}$$

$$=\frac{Zq\mu_0}{L}\frac{n\left(V_{ds}\right)}{1-\frac{\mu_0}{\beta\upsilon_F L}\left\{\frac{\alpha}{\beta}H_1+H_2\right\}}+\frac{\mu_0}{\beta\upsilon_F L}\left(\frac{\sqrt{n\left(V_{ds}\right)}+\frac{\alpha}{\beta}n\left(V_{ds}\right)}{1-\frac{\mu_0}{\beta\upsilon_F L}\left\{\frac{\alpha}{\beta}H_1+H_2\right\}}\right)\frac{\frac{Zq\mu_0}{L}H_1}{1-\frac{\mu_0}{\beta\upsilon_F L}\left\{\frac{\alpha}{\beta}H_1+H_2\right\}}$$

$$=\frac{Zq\mu_0}{L}\frac{n\left(V_{ds}\right)}{1-\frac{\mu_0}{\beta\upsilon_F L}\left\{\frac{\alpha}{\beta}H_1+H_2\right\}}+\frac{\mu_0}{\beta\upsilon_F L}I_D\frac{\sqrt{n\left(V_{ds}\right)}+\frac{\alpha}{\beta}n\left(V_{ds}\right)}{1-\frac{\mu_0}{\beta\upsilon_F L}\left\{\frac{\alpha}{\beta}H_1+H_2\right\}}$$

$$=\frac{Zq\mu_0}{L}\left\{\frac{n\left(V_{ds}\right)+\frac{I_D}{Zq\beta\upsilon_F}\left\{\sqrt{n\left(V_{ds}\right)}+\frac{\alpha}{\beta}n\left(V_{ds}\right)\right\}}{1-\frac{\mu_0}{\beta\upsilon_F L}\left\{\frac{\alpha}{\beta}H_1+H_2\right\}}\right\}$$

$$\Rightarrow \frac{d}{dV_{ds}}\frac{\frac{Zq\mu_0}{L}\int_0^{V_{ds}} n(V)\,dV}{1-\frac{\mu_0}{\beta\upsilon_F L}\left\{\int_0^{V_{ds}}\sqrt{n(V)}dV+\frac{\alpha}{\beta}\int_0^{V_{ds}} n(V)\,dV\right\}}=\frac{Zq\mu_0}{L}\left\{\frac{n\left(V_{ds}\right)+\frac{I_D}{Zq\beta\upsilon_F}\left\{\sqrt{n\left(V_{ds}\right)}+\frac{\alpha}{\beta}n\left(V_{ds}\right)\right\}}{1-\frac{\mu_0}{\beta\upsilon_F L}\left\{\frac{\alpha}{\beta}H_1+H_2\right\}}\right\} \tag{F-8}$$

$$\Rightarrow \frac{dI_D}{dV_{ds}}=\frac{Zq\mu_0}{L}\left\{\begin{array}{l}\dfrac{n\left(V_{ds}\right)-\frac{I_D}{Zq\beta\upsilon_F}\left\{\sqrt{n\left(V_{ds}\right)}+\frac{\alpha}{\beta}n\left(V_{ds}\right)\right\}}{1+\frac{\mu_0}{\beta\upsilon_F L}\left\{\frac{\alpha}{\beta}H_1+H_2\right\}}\Theta\left(V_{ds}\right)\\ +\dfrac{n\left(V_{ds}\right)+\frac{I_D}{Zq\beta\upsilon_F}\left\{\sqrt{n\left(V_{ds}\right)}+\frac{\alpha}{\beta}n\left(V_{ds}\right)\right\}}{1-\frac{\mu_0}{\beta\upsilon_F L}\left\{\frac{\alpha}{\beta}H_1+H_2\right\}}\Theta\left(-V_{ds}\right)\end{array}\right\} \tag{F-9}$$

INTENTIONALLY LEFT BLANK.

Appendix G. Evaluation of Integrals in Electrical Parameters of Graphene FETS Using The Corrected Model of Meric et al. (No Access Resistance)

Since $n(V)=\sqrt{{n_0}^2+\left(C_{gst}/q\right)^2\left(V-V_0\right)^2}$, we can evaluate the integrals that appear in the FET electrical parameters:

$$H_1=\int_{V_a}^{V_b} n(V)\,dV=\int_{V_a}^{V_b}\sqrt{{n_0}^2+\left(\frac{C_{gst}}{q}\right)^2\left(V-V_{th}\right)^2}\,dV$$

$$V=V_{th}+\left(\frac{n_0 q}{C_{gst}}\right)\sinh\theta\Rightarrow {n_0}^2+\left(\frac{C_{gst}}{q}\right)^2\left(V-V_{th}\right)^2={n_0}^2+\left(\frac{C_{gst}}{q}\right)^2\left(\frac{n_0 q}{C_{gst}}\right)^2\sinh^2\theta$$

$$={n_0}^2\left\{1+\sinh^2\theta\right\}={n_0}^2\cosh^2\theta\Rightarrow\sqrt{{n_0}^2+\left(\frac{C_{gst}}{q}\right)^2\left(V-V_{th}\right)^2}=n_0\cosh\theta$$

$$dV=\left(\frac{n_0 q}{C_{gst}}\right)\cosh\theta d\theta\Rightarrow H_1={n_0}^2\left(\frac{q}{C_{gst}}\right)\int_{\theta_a}^{\theta_b}\cosh^2\theta d\theta=\frac{1}{2}{n_0}^2\left(\frac{q}{C_{gst}}\right)\int_{\theta_a}^{\theta_b}\left[1+\cosh 2\theta\right]d\theta$$

$$=\frac{1}{2}{n_0}^2\left(\frac{q}{C_{gst}}\right)\left[\theta+\sinh\theta\cosh\theta\right]_{\theta_a}^{\theta_b}=\frac{1}{2}{n_0}^2\left(\frac{q}{C_{gst}}\right)\left[\theta_b-\theta_a+\sinh\theta_b\cosh\theta_b-\sinh\theta_a\cosh\theta_a\right]$$

$$=\frac{1}{2}{n_0}^2\left(\frac{q}{C_{gst}}\right)\left[\begin{array}{l}\sinh^{-1}\left(\frac{C_{gst}}{n_0 q}\left[V_b-V_{th}\right]\right)+\left(\frac{C_{gst}}{n_0 q}\left[V_b-V_{th}\right]\right)\sqrt{1+\left(\frac{C_{gst}}{n_0 q}\right)^2\left(V_b-V_{th}\right)^2}\\ -\sinh^{-1}\left(\frac{C_{gst}}{n_0 q}\left[V_a-V_{th}\right]\right)-\left(\frac{C_{gst}}{n_0 q}\left[V_a-V_{th}\right]\right)\sqrt{1+\left(\frac{C_{gst}}{n_0 q}\right)^2\left(V_a-V_{th}\right)^2}\end{array}\right] \qquad \text{(G-1)}$$

Likewise, we have

$$H_2=\int_{V_a}^{V_b}\sqrt{n(V)}dV=\int_{V_a}^{V_b}\left[{n_0}^2+\left(\frac{C_{gst}}{q}\right)^2\left(V-V_{th}\right)^2\right]^{1/4}dV$$

$$V=V_{th}+\left(\frac{n_0 q}{C_{gst}}\right)\sinh\theta\Rightarrow {n_0}^2+\left(\frac{C_{gst}}{q}\right)^2\left(V-V_{th}\right)^2={n_0}^2+\left(\frac{C_{gst}}{q}\right)^2\left(\frac{n_0 q}{C_{gst}}\right)^2\sinh^2\theta={n_0}^2\cosh^2\theta \qquad \text{(G-2)}$$

$$dV=\left(\frac{n_0 q}{C_{gst}}\right)\cosh\theta d\theta\Rightarrow H_1={n_0}^{1/2}\left(\frac{n_0 q}{C_{gst}}\right)\int_{\theta_a}^{\theta_b}\cosh^{3/2}\theta d\theta$$

$$x^2 = \cosh\theta \Rightarrow 2xdx = \sinh\theta d\theta = \sqrt{x^4 - 1}\, d\theta$$

$$\Rightarrow d\theta = \frac{2xdx}{\sqrt{x^4-1}} \Rightarrow \int_{\theta_a}^{\theta_b} \cosh^{3/2}\theta d\theta = 2\int_{\sqrt{\cosh\theta_a}}^{\sqrt{\cosh\theta_b}} \frac{t^4 dt}{\sqrt{t^4-1}} \equiv 2\int_{\tau_a}^{\tau_b} \frac{t^4 dt}{\sqrt{t^4-1}} \tag{G-3}$$

$$t = \frac{1}{\mathrm{cn}(x\,|\,m)} \Rightarrow dt = \frac{\mathrm{sn}(x\,|\,m)\,\mathrm{dn}(x\,|\,m)}{\mathrm{cn}^2(x\,|\,m)}dx \qquad x = \mathrm{cn}^{-1}\left(\frac{1}{t}\,|\,m\right) \Rightarrow \Phi_{a,b} = \mathrm{cn}^{-1}\left(\frac{1}{\tau_{a,b}}\,|\,m\right)$$

$$\frac{t^4}{\sqrt{t^4-1}} = \frac{\mathrm{cn}^{-4}(x\,|\,m)}{\sqrt{\mathrm{cn}^{-4}(x\,|\,m)-1}} = \frac{1}{\mathrm{cn}^2(x\,|\,m)\sqrt{1-\mathrm{cn}^4(x\,|\,m)}} = \frac{1}{\mathrm{cn}^2(x\,|\,m)\sqrt{\left[1-\mathrm{cn}^2(x\,|\,m)\right]\left[1+\mathrm{cn}^2(x\,|\,m)\right]}}$$

$$\Rightarrow \frac{t^4 dt}{\sqrt{t^4-1}} = \frac{1}{\mathrm{cn}^2(x\,|\,m)\,\mathrm{sn}(x\,|\,m)\sqrt{2}\,\mathrm{dn}(x\,|\,m)} \frac{\mathrm{sn}(x\,|\,m)\,\mathrm{dn}(x\,|\,m)}{\mathrm{cn}^2(x\,|\,m)}dx = \frac{1}{\sqrt{2}}\frac{dx}{\mathrm{cn}^4(x\,|\,m)}$$

$$\frac{1}{\sqrt{2}}\int_{\Phi_a}^{\Phi_b} \frac{d\theta}{\mathrm{cn}^4\theta} = -\frac{1}{3m_1}\frac{1}{\sqrt{2}}\left[-\frac{\mathrm{sn}\Phi_b\,\mathrm{dn}\Phi_b}{\mathrm{cn}^3\Phi_b} + \frac{\mathrm{sn}\Phi_a\,\mathrm{dn}\Phi_a}{\mathrm{cn}^3\Phi_a} - 2(1-2m)\int_{\Phi_a}^{\Phi_b}\frac{d\theta}{\mathrm{cn}^2\theta} - m\left(\Phi_b - \Phi_a\right)\right]$$

$$= \frac{1}{3m_1}\frac{1}{\sqrt{2}}\left[\frac{\mathrm{sn}\Phi_b\,\mathrm{dn}\Phi_b}{\mathrm{cn}^3\Phi_b} - \frac{\mathrm{sn}\Phi_a\,\mathrm{dn}\Phi_a}{\mathrm{cn}^3\Phi_a} + 2(1-2m)\int_{\Phi_a}^{\Phi_b}\frac{d\theta}{\mathrm{cn}^2\theta} + m\left(\Phi_b - \Phi_a\right)\right]$$

$$m = m_1 = \frac{1}{2} \Rightarrow \frac{1}{\sqrt{2}}\int_{\Phi_a}^{\Phi_b}\frac{d\theta}{\mathrm{cn}^4\theta} = \frac{2}{3\sqrt{2}}\left[\frac{\mathrm{sn}\Phi_b\,\mathrm{dn}\Phi_b}{\mathrm{cn}^3\Phi_b} - \frac{\mathrm{sn}\Phi_a\,\mathrm{dn}\Phi_a}{\mathrm{cn}^3\Phi_a} + \frac{1}{2}\left(\Phi_b - \Phi_a\right)\right] \tag{G-4}$$

$$\mathrm{cn}\Phi_{a,b} = \frac{1}{\tau_{a,b}} = \sqrt{\mathrm{sech}\theta_{a,b}}$$

$$\mathrm{sn}\Phi_{a,b} = \sqrt{1-\mathrm{cn}^2\Phi_{a,b}} = \sqrt{1-\frac{1}{\tau_{a,b}^2}} = \sqrt{1-\mathrm{sech}\theta_{a,b}} \tag{G-5}$$

$$\mathrm{dn}\Phi_{a,b} = \sqrt{m_1 + m\mathrm{cn}^2\Phi_{a,b}} = \sqrt{\frac{1}{2}\left(1+\mathrm{cn}^2\Phi_{a,b}\right)} = \sqrt{\frac{1}{2}\left(1+\frac{1}{\tau_{a,b}^2}\right)} = \sqrt{\frac{1}{2}\left(1+\mathrm{sech}\theta_{a,b}\right)}$$

$$\Rightarrow \mathrm{sn}\Phi_{a,b}\,\mathrm{dn}\Phi_{a,b} = \sqrt{\frac{1}{2}\left(1-\mathrm{sech}^2\theta_{a,b}\right)} = \frac{1}{\sqrt{2}}\tanh\theta_{a,b}$$

$$\Rightarrow \frac{\mathrm{sn}\Phi_{a,b}\,\mathrm{dn}\Phi_{a,b}}{\mathrm{cn}^3\Phi_{a,b}} = \frac{\frac{1}{\sqrt{2}}\tanh\theta_{a,b}}{\mathrm{sech}\theta_{a,b}\sqrt{\mathrm{sech}\theta_{a,b}}} = \frac{1}{\sqrt{2}}\sinh\theta_{a,b}\sqrt{\cosh\theta_{a,b}} \tag{G-6}$$

$$\Rightarrow H_2 = n_0^{1/2}\left(\frac{n_0 q}{C_{gst}}\right)\int_{\Phi_a}^{\Phi_b}\frac{d\theta}{\mathrm{cn}^4\theta} = \frac{1}{3\sqrt{2}}n_0^{1/2}\left(\frac{n_0 q}{C_{gst}}\right)\begin{bmatrix}\sqrt{2}\sinh\theta_b\sqrt{\cosh\theta_b} - \sqrt{2}\sinh\theta_a\sqrt{\cosh\theta_a}\\ +\mathrm{cn}^{-1}\sqrt{\mathrm{sech}\theta_b} - \mathrm{cn}^{-1}\sqrt{\mathrm{sech}\theta_a}\end{bmatrix}$$

$$= \frac{1}{3}n_0^{1/2}\left(\frac{n_0 q}{C_{gst}}\right)\begin{bmatrix}\sinh\theta_b\sqrt{\cosh\theta_b} - \sinh\theta_a\sqrt{\cosh\theta_a}\\ +\frac{1}{\sqrt{2}}\mathrm{cn}^{-1}\sqrt{\mathrm{sech}\theta_b} - \frac{1}{\sqrt{2}}\mathrm{cn}^{-1}\sqrt{\mathrm{sech}\theta_a}\end{bmatrix}$$

INTENTIONALLY LEFT BLANK.

Appendix H. Small Signal Parameters for Graphene FETS Using the Corrected Model of Meric et al. (No Access Resistance)

We already have the output conductance:

$$s_d = \frac{dI_D}{dV_{ds}} = \frac{Zq\mu_0}{L}\left\{\begin{array}{l} \dfrac{n\left(V_{ds}\right) - \dfrac{I_D}{Zq\beta\upsilon_F}\left\{\sqrt{n\left(V_{ds}\right)} + \dfrac{\alpha}{\beta}n\left(V_{ds}\right)\right\}}{1 + \dfrac{\mu_0}{\beta\upsilon_F L}\left\{\dfrac{\alpha}{\beta}H_1 + H_2\right\}}\Theta\left(V_D\right) \\ + \dfrac{n\left(V_{ds}\right) + \dfrac{I_D}{Zq\beta\upsilon_F}\left\{\sqrt{n\left(V_{ds}\right)} + \dfrac{\alpha}{\beta}n\left(V_{ds}\right)\right\}}{1 - \dfrac{\mu_0}{\beta\upsilon_F L}\left\{\dfrac{\alpha}{\beta}H_1 + H_2\right\}}\Theta\left(-V_D\right) \end{array}\right\} \qquad \text{(H-1)}$$

$$= \frac{Zq\upsilon_F n\left(V_{ds}\right) - \dfrac{1}{\beta}\left\{\sqrt{n\left(V_{ds}\right)} + \dfrac{\alpha}{\beta}n\left(V_{ds}\right)\right\}\left|I_D\right|}{\dfrac{\upsilon_F L}{\mu_0} + \dfrac{1}{\beta}\left|H_2 + \dfrac{\alpha}{\beta}H_1\right|}$$

For the transconductance we proceed as before:

$$I_D = \frac{\dfrac{Zq\mu_0}{L}\int_0^{V_{ds}} n\left(V, V_{gst}\right)dV}{1 + \dfrac{\mu_0}{\beta\upsilon_F L}\left|\int_0^{V_{ds}}\sqrt{n\left(V, V_{gst}\right)}dV + \dfrac{\alpha}{\beta}\int_0^{V_{ds}} n\left(V, V_{gst}\right)dV\right|} \qquad \text{(H-2)}$$

$$g_m = \frac{dI_D}{dV_{gst}} = \frac{d}{dV_{gst}}\frac{\dfrac{Zq\mu_0}{L}\int_0^{V_{ds}} n\left(V, V_{gst}\right)dV}{1 + \dfrac{\mu_0}{\beta\upsilon_F L}\left|\int_0^{V_{ds}}\sqrt{n\left(V, V_{gst}\right)}dV + \dfrac{\alpha}{\beta}\int_0^{V_{ds}} n\left(V, V_{gst}\right)dV\right|} \qquad \text{(H-3)}$$

$$= \frac{d}{dV_{gst}} \left\{ \begin{array}{l} \dfrac{\dfrac{Zq\mu_0}{L} \int_0^{V_{ds}} n\left(V, V_{gst}\right) dV}{1 + \dfrac{\mu_0}{\beta \upsilon_F L} \left\{ \int_0^{V_{ds}} \sqrt{n\left(V, V_{gst}\right)} dV + \dfrac{\alpha}{\beta} \int_0^{V_{ds}} n\left(V, V_{gst}\right) dV \right\}} \Theta\left(V_{ds}\right) \\ + \dfrac{\dfrac{Zq\mu_0}{L} \int_0^{V_{ds}} n(V) dV}{1 - \dfrac{\mu_0}{\beta \upsilon_F L} \left\{ \int_0^{V_{ds}} \sqrt{n\left(V, V_{gst}\right)} dV + \dfrac{\alpha}{\beta} \int_0^{V_{ds}} n\left(V, V_{gst}\right) dV \right\}} \Theta\left(-V_{ds}\right) \end{array} \right\} \quad \text{(H-4)}$$

$$= \left\{ \begin{array}{l} \Theta\left(V_{ds}\right) \dfrac{d}{dV_{gst}} \dfrac{\dfrac{Zq\mu_0}{L} \int_0^{V_{ds}} n\left(V, V_{gst}\right) dV}{1 + \dfrac{\mu_0}{\beta \upsilon_F L} \left\{ \int_0^{V_D} \sqrt{n\left(V, V_{gst}\right)} dV + \dfrac{\alpha}{\beta} \int_0^{V_D} n\left(V, V_{gst}\right) dV \right\}} \\ + \Theta\left(-V_{ds}\right) \dfrac{d}{dV_{gst}} \dfrac{\dfrac{Zq\mu_0}{L} \int_0^{V_{ds}} n\left(V, V_{gt}\right) dV}{1 - \dfrac{\mu_0}{\beta \upsilon_F L} \left\{ \int_0^{V_{ds}} \sqrt{n\left(V, V_{gst}\right)} dV + \dfrac{\alpha}{\beta} \int_0^{V_{ds}} n\left(V, V_{gst}\right) dV \right\}} \end{array} \right\} \quad \text{(H-5)}$$

$$\frac{d}{dV_{gst}} \frac{\dfrac{Zq\mu_0}{L} \int_0^{V_{ds}} n\left(V, V_{gst}\right) dV}{1 + \dfrac{\mu_0}{\beta \upsilon_F L} \left\{ \int_0^{V_D} \sqrt{n\left(V, V_{gst}\right)} dV + \dfrac{\alpha}{\beta} \int_0^{V_D} n\left(V, V_{gst}\right) dV \right\}} = \frac{\dfrac{Zq\mu_0}{L} \int_0^{V_{ds}} \dfrac{d}{dV_{gst}} n\left(V, V_{gst}\right) dV}{1 + \dfrac{\mu_0}{\beta \upsilon_F L} \left\{ \int_0^{V_{ds}} \sqrt{n\left(V, V_{gst}\right)} dV + \dfrac{\alpha}{\beta} \int_0^{V_{ds}} n\left(V, V_{gst}\right) dV \right\}} \quad \text{(H-6)}$$

$$+ \frac{Zq\mu_0}{L} \int_0^{V_{ds}} n\left(V, V_{gst}\right) dV \cdot \frac{d}{dV_{gst}} \frac{1}{1 + \dfrac{\mu_0}{\beta \upsilon_F L} \left\{ \int_0^{V_{ds}} \sqrt{n\left(V, V_{gst}\right)} dV + \dfrac{\alpha}{\beta} \int_0^{V_{ds}} n\left(V, V_{gst}\right) dV \right\}}$$

$$= \frac{\dfrac{Zq\mu_0}{L}\int_0^{V_{ds}} \dfrac{d}{dV_{gst}} n\left(V,V_{gst}\right)dV}{1+\dfrac{\mu_0}{\beta\upsilon_F L}\left\{\int_0^{V_{ds}} \sqrt{n\left(V,V_{gst}\right)}dV + \dfrac{\alpha}{\beta}\int_0^{V_{ds}} n\left(V,V_{gst}\right)dV\right\}}$$

$$-\frac{Zq\mu_0}{L}\int_0^{V_{ds}} n\left(V,V_{gst}\right)dV \cdot \frac{\dfrac{\mu_0}{\beta\upsilon_F L}\left\{\int_0^{V_{ds}} \dfrac{d}{dV_{gst}}\sqrt{n\left(V,V_{gst}\right)}dV + \dfrac{\alpha}{\beta}\int_0^{V_{ds}} \dfrac{d}{dV_{gst}} n\left(V,V_{gst}\right)dV\right\}}{\left[1+\dfrac{\mu_0}{\beta\upsilon_F L}\left\{\int_0^{V_{ds}} \sqrt{n\left(V,V_{gst}\right)}dV + \dfrac{\alpha}{\beta}\int_0^{V_{ds}} n\left(V,V_{gst}\right)dV\right\}\right]^2} \quad \text{(H-7)}$$

$$n(V,V_{gst}) = \sqrt{{n_0}^2 + \left(C_{gst}/q\right)^2\left(V - V_{gst} - V_{th}\right)^2} \Rightarrow \begin{cases} \dfrac{d}{dV_{gst}} n(V,V_{gst}) = -\dfrac{d}{dV} n(V,V_{gst}) \\ \dfrac{d}{dV_{gst}}\sqrt{n(V,V_{gst})} = -\dfrac{d}{dV}\sqrt{n(V,V_{gst})} \end{cases} \quad \text{(H-8)}$$

$$\Rightarrow \frac{d}{dV_{gst}}\frac{\dfrac{Zq\mu_0}{L}\int_0^{V_{ds}} n\left(V,V_{gst}\right)dV}{1+\dfrac{\mu_0}{\beta\upsilon_F L}\left\{\int_0^{V_{ds}} \sqrt{n\left(V,V_{gst}\right)}dV + \dfrac{\alpha}{\beta}\int_0^{V_{ds}} n\left(V,V_{gst}\right)dV\right\}} = \frac{-\dfrac{Zq\mu_0}{L}\int_0^{V_{ds}} \dfrac{d}{dV} n\left(V,V_{gst}\right)dV}{1+\dfrac{\mu_0}{\beta\upsilon_F L}\left\{\int_0^{V_{ds}} \sqrt{n\left(V,V_{gst}\right)}dV + \dfrac{\alpha}{\beta}\int_0^{V_{ds}} n\left(V,V_{gst}\right)dV\right\}} \quad \text{(H-9)}$$

$$+\frac{Zq\mu_0}{L}\int_0^{V_{ds}} n\left(V,V_{gst}\right)dV \cdot \frac{\dfrac{\mu_0}{\beta\upsilon_F L}\left\{\int_0^{V_{ds}} \dfrac{d}{dV}\sqrt{n\left(V,V_{gst}\right)}dV + \dfrac{\alpha}{\beta}\int_0^{V_{ds}} \dfrac{d}{dV} n\left(V,V_{gst}\right)dV\right\}}{\left[1+\dfrac{\mu_0}{\beta\upsilon_F L}\left\{\int_0^{V_{ds}} \sqrt{n\left(V,V_{gst}\right)}dV + \dfrac{\alpha}{\beta}\int_0^{V_{ds}} n\left(V,V_{gst}\right)dV\right\}\right]^2}$$

$$= \frac{-\frac{Zq\mu_0}{L}\left[n\left(V_{ds},V_{gst}\right)-n\left(0,V_{gst}\right)\right]}{1+\frac{\mu_0}{\beta\upsilon_F L}\left\{\int_0^{V_{ds}}\sqrt{n\left(V,V_{gst}\right)}dV+\frac{\alpha}{\beta}\int_0^{V_{ds}}n\left(V,V_{gst}\right)dV\right\}}+\frac{Zq\mu_0}{L}\int_0^{V_{ds}}n\left(V,V_{gst}\right)dV$$

$$\cdot\frac{\frac{\mu_0}{\beta\upsilon_F L}\left\{\sqrt{n\left(V_{ds},V_{gst}\right)}-\sqrt{n\left(0,V_{gst}\right)}+\frac{\alpha}{\beta}\left[n\left(V_{ds},V_{gst}\right)-n\left(0,V_{gst}\right)\right]\right\}}{\left[1+\frac{\mu_0}{\beta\upsilon_F L}\left\{\int_0^{V_{ds}}\sqrt{n\left(V,V_{gst}\right)}dV+\frac{\alpha}{\beta}\int_0^{V_{ds}}n\left(V,V_{gst}\right)dV\right\}\right]^2}$$

$$= \frac{-\frac{Zq\mu_0}{L}\left[n\left(V_{ds},V_{gst}\right)-n\left(0,V_{gst}\right)\right]}{1+\frac{\mu_0}{\beta\upsilon_F L}\left\{\int_0^{V_{ds}}\sqrt{n\left(V,V_{gst}\right)}dV+\frac{\alpha}{\beta}\int_0^{V_{ds}}n\left(V,V_{gst}\right)dV\right\}}$$

$$+\frac{\frac{\mu_0}{\beta\upsilon_F L}\left\{\sqrt{n\left(V_{ds},V_{gst}\right)}-\sqrt{n\left(0,V_{gst}\right)}+\frac{\alpha}{\beta}\left[n\left(V_{ds},V_{gst}\right)-n\left(0,V_{gst}\right)\right]\right\}I_D}{1+\frac{\mu_0}{\beta\upsilon_F L}\left\{\int_0^{V_{ds}}\sqrt{n\left(V,V_{gst}\right)}dV+\frac{\alpha}{\beta}\int_0^{V_{ds}}n\left(V,V_{gst}\right)dV\right\}} \qquad \text{(H-10)}$$

$$= \frac{\frac{\mu_0}{\beta\upsilon_F L}\left\{\sqrt{n\left(V_{ds},V_{gst}\right)}-\sqrt{n\left(0,V_{gst}\right)}+\frac{\alpha}{\beta}\left[n\left(V_{ds},V_{gst}\right)-n\left(0,V_{gst}\right)\right]\right\}I_D-\frac{Zq\mu_0}{L}\left[n\left(V_{ds},V_{gst}\right)-n\left(0,V_{gst}\right)\right]}{1+\frac{\mu_0}{\beta\upsilon_F L}\left\{H_2+\frac{\alpha}{\beta}H_1\right\}}$$

$$\frac{d}{dV_{gst}}\frac{\frac{Zq\mu_0}{L}\int_0^{V_{ds}}n\left(V,V_{gst}\right)dV}{1-\frac{\mu_0}{\beta\upsilon_F L}\left\{\int_0^{V_{ds}}\sqrt{n\left(V,V_{gst}\right)}dV+\frac{\alpha}{\beta}\int_0^{V_{ds}}n\left(V,V_{gst}\right)dV\right\}}=\frac{\frac{Zq\mu_0}{L}\int_0^{V_{ds}}\frac{d}{dV_{gst}}n\left(V,V_{gst}\right)dV}{1-\frac{\mu_0}{\beta\upsilon_F L}\left\{\int_0^{V_{ds}}\sqrt{n\left(V,V_{gst}\right)}dV+\frac{\alpha}{\beta}\int_0^{V_{ds}}n\left(V,V_{gst}\right)dV\right\}} \qquad \text{(H-11)}$$

$$+\frac{Zq\mu_0}{L}\int_0^{V_{ds}}n\left(V,V_{gst}\right)dV\cdot\frac{d}{dV_{gst}}\frac{1}{1-\frac{\mu_0}{\beta\upsilon_F L}\left\{\int_0^{V_{ds}}\sqrt{n\left(V,V_{gst}\right)}dV+\frac{\alpha}{\beta}\int_0^{V_{ds}}n\left(V,V_{gst}\right)dV\right\}}$$

$$= \frac{\dfrac{Zq\mu_0}{L}\int_0^{V_{ds}} \dfrac{d}{dV_{gst}} n\left(V, V_{gst}\right) dV}{1 - \dfrac{\mu_0}{\beta \upsilon_F L}\left\{\int_0^{V_{ds}} \sqrt{n\left(V, V_{gst}\right)}\, dV + \dfrac{\alpha}{\beta}\int_0^{V_{ds}} n\left(V, V_{gst}\right) dV\right\}}$$

$$+ \frac{Zq\mu_0}{L}\int_0^{V_{ds}} n\left(V, V_{gst}\right) dV \cdot \frac{\dfrac{\mu_0}{\beta \upsilon_F L}\left\{\int_0^{V_{ds}} \dfrac{d}{dV_{gst}}\sqrt{n\left(V, V_{gst}\right)}\, dV + \dfrac{\alpha}{\beta}\int_0^{V_{ds}} \dfrac{d}{dV_{gst}} n\left(V, V_{gst}\right) dV\right\}}{\left[1 - \dfrac{\mu_0}{\beta \upsilon_F L}\left\{\int_0^{V_{ds}} \sqrt{n\left(V, V_{gst}\right)}\, dV + \dfrac{\alpha}{\beta}\int_0^{V_{ds}} n\left(V, V_{gst}\right) dV\right\}\right]^2} \qquad \text{(H-12)}$$

$$n(V, V_{gst}) = \sqrt{{n_0}^2 + \left(C_{gst}/q\right)^2 \left(V - V_{gst} - V_{th}\right)^2} \Rightarrow \begin{cases} \dfrac{d}{dV_{gst}} n(V, V_{gst}) = -\dfrac{d}{dV} n(V, V_{gst}) \\ \dfrac{d}{dV_{gst}}\sqrt{n(V, V_{gst})} = -\dfrac{d}{dV}\sqrt{n(V, V_{gst})} \end{cases} \qquad \text{(H-13)}$$

$$\Rightarrow \frac{d}{dV_{gst}} \frac{\dfrac{Zq\mu_0}{L}\int_0^{V_{ds}} n\left(V, V_{gst}\right) dV}{1 - \dfrac{\mu_0}{\beta \upsilon_F L}\left\{\int_0^{V_{ds}} \sqrt{n\left(V, V_{gst}\right)}\, dV + \dfrac{\alpha}{\beta}\int_0^{V_{ds}} n\left(V, V_{gst}\right) dV\right\}} = \frac{-\dfrac{Zq\mu_0}{L}\int_0^{V_{ds}} \dfrac{d}{dV} n\left(V, V_{gst}\right) dV}{1 - \dfrac{\mu_0}{\beta \upsilon_F L}\left\{\int_0^{V_{ds}} \sqrt{n\left(V, V_{gst}\right)}\, dV + \dfrac{\alpha}{\beta}\int_0^{V_{ds}} n\left(V, V_{gst}\right) dV\right\}} \qquad \text{(H-14)}$$

$$- \frac{Zq\mu_0}{L}\int_0^{V_{ds}} n\left(V, V_{gst}\right) dV \cdot \frac{\dfrac{\mu_0}{\beta \upsilon_F L}\left\{\int_0^{V_{ds}} \dfrac{d}{dV}\sqrt{n\left(V, V_{gst}\right)}\, dV + \dfrac{\alpha}{\beta}\int_0^{V_{ds}} \dfrac{d}{dV} n\left(V, V_{gst}\right) dV\right\}}{\left[1 - \dfrac{\mu_0}{\beta \upsilon_F L}\left\{\int_0^{V_{ds}} \sqrt{n\left(V, V_{gst}\right)}\, dV + \dfrac{\alpha}{\beta}\int_0^{V_{ds}} n\left(V, V_{gst}\right) dV\right\}\right]^2}$$

$$= \frac{-\frac{Zq\mu_0}{L}\left[n\left(V_{ds},V_{gst}\right)-n\left(0,V_{gst}\right)\right]}{1-\frac{\mu_0}{\beta\upsilon_F L}\left\{\int_0^{V_{ds}}\sqrt{n\left(V,V_{gst}\right)}dV+\frac{\alpha}{\beta}\int_0^{V_{ds}}n\left(V,V_{gst}\right)dV\right\}}-\frac{Zq\mu_0}{L}\int_0^{V_{ds}}n\left(V,V_{gst}\right)dV$$

$$\cdot\frac{\frac{\mu_0}{\beta\upsilon_F L}\left\{\sqrt{n\left(V_{ds},V_{gst}\right)}-\sqrt{n\left(0,V_{gst}\right)}+\frac{\alpha}{\beta}\left[n\left(V_{ds},V_{gst}\right)-n\left(0,V_{gst}\right)\right]\right\}}{\left[1-\frac{\mu_0}{\beta\upsilon_F L}\left\{\int_0^{V_{ds}}\sqrt{n\left(V,V_{gst}\right)}dV+\frac{\alpha}{\beta}\int_0^{V_{ds}}n\left(V,V_{gst}\right)dV\right\}\right]^2}$$

$$= \frac{-\frac{Zq\mu_0}{L}\left[n\left(V_{ds},V_{gst}\right)-n\left(0,V_{gst}\right)\right]}{1-\frac{\mu_0}{\beta\upsilon_F L}\left\{\int_0^{V_{ds}}\sqrt{n\left(V,V_{gst}\right)}dV+\frac{\alpha}{\beta}\int_0^{V_{ds}}n\left(V,V_{gst}\right)dV\right\}}-\frac{\frac{\mu_0}{\beta\upsilon_F L}\left\{\sqrt{n\left(V_{ds},V_{gst}\right)}-\sqrt{n\left(0,V_{gst}\right)}+\frac{\alpha}{\beta}\left[n\left(V_{ds},V_{gst}\right)-n\left(0,V_{gst}\right)\right]\right\}I_D}{1-\frac{\mu_0}{\beta\upsilon_F L}\left\{\int_0^{V_{ds}}\sqrt{n\left(V,V_{gst}\right)}dV+\frac{\alpha}{\beta}\int_0^{V_{ds}}n\left(V,V_{gst}\right)dV\right\}}$$

$$= \frac{-\frac{\mu_0}{\beta\upsilon_F L}\left\{\sqrt{n\left(V_{ds},V_{gst}\right)}-\sqrt{n\left(0,V_{gst}\right)}+\frac{\alpha}{\beta}\left[n\left(V_{ds},V_{gst}\right)-n\left(0,V_{gst}\right)\right]\right\}I_D-\frac{Zq\mu_0}{L}\left[n\left(V_{ds},V_{gst}\right)-n\left(0,V_{gst}\right)\right]}{1-\frac{\mu_0}{\beta\upsilon_F L}\left\{H_2+\frac{\alpha}{\beta}H_1\right\}} \qquad \text{(H-15)}$$

so the final form is

$$g_m = \left\{\begin{array}{l}\dfrac{\frac{\mu_0}{\beta\upsilon_F L}\left\{\sqrt{n\left(V_{ds},V_{gst}\right)}-\sqrt{n\left(0,V_{gst}\right)}+\frac{\alpha}{\beta}\left[n\left(V_{ds},V_{gst}\right)-n\left(0,V_{gst}\right)\right]\right\}I_D-\frac{Zq\mu_0}{L}\left[n\left(V_{ds},V_{gst}\right)-n\left(0,V_{gst}\right)\right]}{1+\frac{\mu_0}{\beta\upsilon_F L}\left\{H_2+\frac{\alpha}{\beta}H_1\right\}}\Theta\left(V_{ds}\right) \\ +\dfrac{-\frac{\mu_0}{\beta\upsilon_F L}\left\{\sqrt{n\left(V_{ds},V_{gst}\right)}-\sqrt{n\left(0,V_{gst}\right)}+\frac{\alpha}{\beta}\left[n\left(V_{ds},V_{gst}\right)-n\left(0,V_{gst}\right)\right]\right\}I_D-\frac{Zq\mu_0}{L}\left[n\left(V_{ds},V_{gst}\right)-n\left(0,V_{gst}\right)\right]}{1-\frac{\mu_0}{\beta\upsilon_F L}\left\{H_2+\frac{\alpha}{\beta}H_1\right\}}\Theta\left(-V_{ds}\right)\end{array}\right\}$$

$$= \frac{\mu_0}{\upsilon_F L}\frac{\frac{1}{\beta}\left\{\sqrt{n\left(V_{ds},V_{gst}\right)}-\sqrt{n\left(0,V_{gst}\right)}+\frac{\alpha}{\beta}\left[n\left(V_{ds},V_{gst}\right)-n\left(0,V_{gst}\right)\right]\right\}\left|I_D\right|-Zq\upsilon_F\left[n\left(V_{ds},V_{gst}\right)-n\left(0,V_{gst}\right)\right]}{1+\frac{\mu_0}{\beta\upsilon_F L}\left|H_2+\frac{\alpha}{\beta}H_1\right|} \qquad \text{(H-16)}$$

List of Symbols, Abbreviations, and Acronyms

2-D	two-dimensional
3-D	three-dimensional
AC	alternating current, nonzero frequency
ARL	U.S. Army Research Laboratory
DC	direct current, zero-frequency
FET	field-effect transistor
HEMT	high electron mobility transistor
I-V	current versus voltage
MESFET	metal semiconductor field-effect transistor
MOSFET	metal-oxide semiconductor field-effect transistor
RF	radio frequency

NO. OF COPIES	ORGANIZATION
1 ELECT	ADMNSTR DEFNS TECHL INFO CTR ATTN DTIC OCP 8725 JOHN J KINGMAN RD STE 0944 FT BELVOIR VA 22060-6218
1 CD	OFC OF THE SECY OF DEFNS ATTN ODDRE (R&AT) THE PENTAGON WASHINGTON DC 20301-3080
1	US ARMY RSRCH DEV AND ENGRG CMND ARMAMENT RSRCH DEV & ENGRG CTR ARMAMENT ENGRG & TECHNLGY CTR ATTN AMSRD AAR AEF T J MATTS BLDG 305 ABERDEEN PROVING GROUND MD 21005-5001
1	PM TIMS, PROFILER (MMS-P) AN/TMQ-52 ATTN B GRIFFIES BUILDING 563 FT MONMOUTH NJ 07703
1	US ARMY ARDEC ATTN AMSRD AAR AEE P C HAINES BLDG 25 PICATINNY ARSENAL NJ 07806-5000
1	US ARMY ARDEC ATTN AMSRD AAR AEM C A MARSTON BLDG 61S PICATINNY ARSENAL NJ 07806-5000
3	US ARMY ARDEC ATTN AMSRD AAR AEM L S GILMAN ATTN AMSRD AAR AEP F O NGUYEN ATTN AMSRD AAR AEP F S SHRI BLDG 65S PICATINNY ARSENAL NJ 07806-5000
1	US ARMY INFO SYS ENGRG CMND ATTN AMSEL IE TD A RIVERA FT HUACHUCA AZ 85613-5300

NO. OF COPIES	ORGANIZATION
1	COMMANDER US ARMY RDECOM ATTN AMSRD AMR W C MCCORKLE 5400 FOWLER RD REDSTONE ARSENAL AL 35898-5000
1	US GOVERNMENT PRINT OFF DEPOSITORY RECEIVING SECTION ATTN MAIL STOP IDAD J TATE 732 NORTH CAPITOL ST NW WASHINGTON DC 20402
1	DEPT OF PHYSICS AND GEOLOGY UNIV OF TEXAS - PAN AMERICAN ATTN S TIDROW 1201 W UNIVERSITY DR EDINBURG TX 78541
1	US ARMY RSRCH LAB ATTN RDRL CIM G T LANDFRIED BLDG 4600 ABERDEEN PROVING GROUND MD 21005-5066
37	US ARMY RSRCH LAB ATTN IMNE ALC HRR MAIL & RECORDS MGMT ATTN RDRL SER L O NAYFEH ATTN RDRL CIM L TECHL LIB ATTN RDRL CIM P TECHL PUB ATTN RDRL D ATTN RDRL SE J PELLEGRINO ATTN RDRL SED E D KATSIS ATTN RDRL SED E K A JONES ATTN RDRL SEE I S SVENSSON ATTN RDRL SEE O W M GOLDING ATTN RDRL SER E B HUEBSCHMAN ATTN RDRL SER E E VIVEIROS ATTN RDRL SER E F CROWNE (10 COPIES) ATTN RDRL SER E G BIRDWELL ATTN RDRL SER E R DEL ROSARIO ATTN RDRL SER E T IVANOV ATTN RDRL SER J MAIT ATTN RDRL SER L B NICHOLS ATTN RDRL SER L C ANTON ATTN RDRL SER L L CURRANO ATTN RDRL SER L M CHIN ATTN RDRL SER L M DUBEY ATTN RDRL SER L M ERVIN ATTN RDRL SER L R POLCAWICH

NO. OF
COPIES ORGANIZATION

ATTN RDRL SER L S KILPATRICK
ATTN RDRL SER M J TATUM
ATTN RDRL SER P AMIRTHARAJ
ATTN RDRL SER U C FAZI
ADELPHI MD 20783-1197

TOTAL: 51 (49 HCS, 1 ELECT, 1 CD)

INTENTIONALLY LEFT BLANK.